

**Simulation Approach to Estimate Rice Yield and Energy Generation  
under Agrivoltaic System**

By

**Thum Chun Hau**

Submitted to the

Graduate School of Agricultural and Life Sciences

The University of Tokyo

in Partial Fulfilment of

the Requirements for the Degree of Master of Science

in

Agricultural Sciences

Principal Supervisor  
Professor Kensuke Okada

2019

## **ACKNOWLEDGEMENT**

I am grateful to many people in writing this Master thesis.

First, I would like to thank my supervisor, Prof. Kensuke Okada for his continuously guidance, enthusiasm, and devotion. His excellent knowledge in academic and remarkable erudition are gratefully acknowledged. My special thanks to Prof. Mizoguchi Masaru and Assoc. Prof. Kae Miyazawa for reviewing my thesis and valuable comments.

Second, my gratitude is expressed to Mr. Kenji Watanabe for numerous supports and his collaboration to the experiment. I am very thankful to Ms. Slavka Batorova and Mr. Ken Matsuoka for introducing rice farmer to me, and explanation on the agrivoltaic system design.

I also want to express my deep gratitude to my friends, laboratory members, and family members for their attention and endless support.

Finally, my deep thanks to my father, mother, and my wife. Their love and support to me will cherish forever.

# Table of Contents

Chapter 1: Introduction .....	11
1.1 Agrivoltaic concept.....	11
1.2 Agrivoltaic system in Japan .....	11
1.3 Rice ( <i>Oryza sativa</i> ) the most important cereal crop in Japan .....	12
1.4 Energy demand in Japan .....	12
1.5 Feed-in Tariff scheme in Japan.....	13
1.6 Agrivoltaic research around the world and in Japan.....	13
1.7 Movable solar photovoltaic panels in AV research .....	15
1.8 Selection of rice in AV research .....	16
1.9 Relationship between solar radiation and rice yield .....	16
1.10 Research objective .....	18
Chapter 2: Effect of partial shading on rice grain yield and energy output.....	19
2.1 Introduction.....	19
2.2 Materials and methods .....	19
2.2.1 Site description.....	19
2.2.2 Experimental plot.....	19
2.2.3 Crop management .....	22
2.2.4 Weather measurement.....	24
2.2.5 Plant growth measurement.....	25
2.2.6 Combine plot yield.....	29
2.2.7 Solar photovoltaic system .....	29
2.3 Results.....	31
2.3.1 Weather conditions .....	31
2.3.2 Dry matter production, leaf area index (LAI) and SPAD value .....	34
2.3.3 Grain yield and total biomass .....	36
2.3.4 Combine plot yield.....	38

2.3.5 Culm length, head length and head number.....	39
2.3.6 Energy output from solar photovoltaic system .....	39
2.4 Discussions .....	40
2.5 Conclusion .....	40
Chapter 3: Calibration and validation of models for light distribution, rice growth and power generation in AV system.....	41
3.1 Introduction.....	41
3.2 Solar radiation model .....	41
3.2.1 Materials and methods: Model calibration and validation for Autodesk Revit and Dynamo.....	42
3.2.2 Results and discussion .....	45
3.3 Crop growth model .....	45
3.3.1 Model parameterization, calibration and validation for APSIM-Oryza .....	45
3.3.2 Materials and methods .....	46
3.3.3 Methods of model evaluation.....	51
3.3.4 Results and discussion .....	52
3.4 Solar energy model .....	54
3.4.1 Materials and methods: model calibration and validation for PVSyst .....	55
3.4.2 Results and discussion .....	55
3.5 Conclusion .....	57
Chapter 4: Scenarios analysis for economically optimum rice and energy production in agrivoltaic system .....	58
4.1 Introduction.....	58
4.2 Scenario analysis of solar radiation at different tilt angles .....	59
4.2.1 Materials and methods .....	59
4.2.2 Results and discussion .....	59
4.3 Scenario analysis of rice yield at different tilt angles .....	60
4.3.1 Materials and methods .....	60

4.3.2 Results and discussion .....	60
4.4 Scenario analysis of energy output at different tilt angles .....	62
4.4.1 Materials and methods .....	62
4.4.2 Results & discussion .....	65
4.5 Economically optimum rice and energy production .....	66
4.6 Conclusion .....	68
Chapter 5: General discussion and conclusion .....	69
5.1 Partial shading on rice yield in AV .....	69
5.2 Simulation approach in AV with rice cultivation .....	69
5.3 Conclusion .....	70
5.4 Recommendations and future study application .....	70

## List of Figures

Figure 1.1 Fixed solar photovoltaic panels in AV system. ....	15
Figure 1.2 Movable solar photovoltaic panels in AV system (Source: <a href="https://solar-sharing-japan.blogspot.com/2014/">https://solar-sharing-japan.blogspot.com/2014/</a> ).....	15
Figure 1.3 Solar radiation requirement of rice at different stages of growth and development (adapted from Stansel, 1975). ....	17
Figure 2.1 Experimental plot in Chikusei city, Ibaraki prefecture. Left: before agrivoltaic system installation, and right: after the installation of agrivoltaic system. (Google earth, downloaded on 1 April 2019) .....	20
Figure 2.2 Schematic layout of agrivoltaic system with environmental sensors (top) and modular structure (bottom). ....	21
Figure 2.3 Agrivoltaic system tilted at 10° (taken on 25 May 2018).....	22
Figure 2.4 (a) Sensors and dataloggers in AV plot. (b) Sensors and dataloggers in OP plot. .	25
Figure 2.5 Sampling locations at harvest (s1 to s6) and delayed harvest (s7 to s12). ....	27
Figure 2.6 a) Sampling in AV plot and b) Sampling in OP plot.....	27
Figure 2.7 Solar Panels and Inverters .....	30
Figure 2.8 Precipitation, maximum and minimum temperature collected from JMA Shimodate Weather Station.....	31
Figure 2.9 Solar radiation collected from JMA Tsukuba Weather Station.....	32
Figure 2.10 Solar radiation collected from experimental field. ....	33
Figure 2.11 Maximum and minimum temperature collected from experimental field.....	33
Figure 2.12: Leaf Area Index (LAI) .....	34
Figure 2.13 Changes of SPAD values during rice growth.....	35
Figure 2.14 Total biomass at different sampling date.....	35
Figure 2.15 Grain yield at different harvest dates.....	36
Figure 2.16 Total biomass at harvest. ....	37
Figure 2.17 Harvest index.....	37
Figure 2.18 Monthly energy output in 2018. ....	39
Figure 3.1 3D views of AV.....	42
Figure 3.2 (a) top view, (b) side view at tilt angle 60°, (c) front view at tilt angle 60°. ....	43
Figure 3.3 Visual programming nodes in Dynamo.....	44
Figure 3.4 3D model with simulation grid size (0.5 m) and tilt angle (10°) in Revit. ....	44

Figure 3.5 Comparison of simulated and observed solar radiation in AV from 2 August to 5 October. Dotted line denotes 1:1 line. ....	45
Figure 3.6 Equations to calculate RMSE and EF. ....	52
Figure 3.7 Observed and simulated total biomass. Dotted line denotes 1:1 line. ....	53
Figure 3.8 Comparison of observed and simulated total biomass at different samplings date. Vertical bars denote the standard error. ....	54
Figure 3.9 Comparison of observed and simulated energy output (kWh). Dotted line denotes 1:1 line. ....	56
Figure 4.1 Solar photovoltaic tilt angle at (a) 14°, (b) 25°, (c) 42°, (d) 60°. ....	60
Figure 4.2 Comparison of simulated grain yield and total biomass at 14°, 25°, 42° and 60° in August. ....	61
Figure 4.3 Difference of simulated grain yield and total biomass at 14°, 25°, 42°, 60° in August. ....	61
Figure 4.4 PVSyst user interface on project designation. ....	63
Figure 4.5 PVSyst user interface on field parameters. ....	64
Figure 4.6 Global system configuration. ....	64
Figure 4.7 Simulated energy output (kWh) at different angles in August. ....	66
Figure 4.8 Total rice and energy income from May to October 2018. ....	67

## List of Tables

Table 2.1 Solar panels tilt angle.....	22
Table 2.2 Crop phenology events .....	23
Table 2.3 Sampling information .....	26
Table 2.4 Solar Photovoltaic System Configuration.....	30
Table 2.5 Grain yield and percentage difference. ....	37
Table 2.6 Comparison of combine plot yield in AV and average rice yield in Chikusei area	38
Table 2.7 Comparison of average rice yield in Chikusei area and combine plot yield in OP	38
Table 2.8 Culm length, head length and head number at harvest .....	39
Table 3.1 Summary of object dimensions used in Revit. ....	42
Table 3.2 Soil Water .....	47
Table 3.3 Initial Nitrogen.....	48
Table 3.4 Soil Organic Matter .....	48
Table 3.5 Phenological Parameter Values for Asahi-no-yume.....	50
Table 3.6 Fraction Dry Matter Partitioned to Storage Organ (FSO) for Rice Cultivar Asahi- no-yume .....	51
Table 3.7 Summary of APSIM-Oryza model performance. ....	53
Table 3.8 Comparison of observed and simulated rice yield and total biomass.....	53
Table 3.9 Solar panels tilt angle.....	55
Table 3.10 Simulated and observed energy output in 2018.....	56
Table 4.1 Solar panels tilt angle.....	58
Table 4.2 Comparison of simulated solar radiation in August .....	59
Table 4.3 Simulated grain yield and rice selling amount.....	62
Table 4.4 Simulated energy output (kWh) at different angles in August. ....	65
Table 4.5 Rice and energy selling amount from May to October 2018.....	67

# **Simulation approach to estimate rice yield and energy generation under agrivoltaic system**

Laboratory of Agricultural Development Studies / IPADS: Thum Chun Hau

Supervisor: Kensuke Okada

## **Introduction:**

Agrivoltaic is the combination of two words, agriculture and photovoltaic that associating solar photovoltaic panels and crop at the same time on the same land area. Agrivoltaic system (AV) was proposed as an innovative solution to solve the competition of land around the years 2000s when many farmers in the US and Europe started to convert their land from food crop to energy crop production due to higher demand of biofuel energy. In Japan, AV became more popular after the introduction of Feed-in Tariff (FIT) scheme in July 2012. This scheme made mandatory for electric utility operator to buy electricity from renewable sources at fixed prices for 10 to 20 years depending on the installed capacity. Many rice farmers on the flat land are attracted to this scheme due to the potential of increasing their income. However, MAFF has enacted a guideline to ensure that crop yield under AV should not decrease more than by 20% when compared to the crop yield in the same area. If so, the AV would be dismantled, and the land should return to purely agriculture activities.

Throughout the literature review up to date, it is understood that accumulation of empirical research on AV is very limited in Japan. Although there are numerous research examples on the influence of insufficient solar radiation on the crop growth, field experiment coupled with modelling study are still lacking. In addition, there are only limited studies which examined the influence of partial shading from solar photovoltaic panels on the rice (shade intolerant) in Japan. Most of the previous studies in AV focused on lettuce, tomato, cucumber, and maize (shade tolerant).

The principal objective of this study is to investigate the effect of rice yield cultivated in an irrigated field under AV in Japan. Then through the use of modelling approaches to simulate solar radiation under AV and its effect on rice yield, the optimum distribution of solar radiation between solar panels and rice crop by adjusting the tilt angle to maximize the monetary income to the AV farm.

## **Materials and methods:**

Field experiment was conducted from May to October in 2018 at a farmer's rice field in Chikusei city, Ibaraki prefecture. Rice cultivar Asahi-no-yume was cultivated under AV. Samplings were collected during crop growth, harvest, and delayed harvest (four and eleven days after normal harvest). Dry matter, grain yield and total biomass were used to calibrate and validate the crop growth model.

In this study, three models were used for simulation, i.e., solar radiation model, crop growth model, and solar energy model. The model used for solar radiation simulation was Autodesk Revit with the integration of visual programming tool in Dynamo. Revit and Dynamo

were used to simulate daily solar radiation under AV and then compare it with observed data. The crop growth model used in this study was APSIM-Oryza. It was used to simulate rice growth in the experimental field and in partial shading condition such as in AV. The third model for solar energy simulation was PVSyst. PVSyst was used to simulate monthly solar energy generation with different tilt angles settings.

## **Results and discussion**

The result from the field experiment indicated partial shading in AV had resulted reduction of grain yield by 22.6% when compared to full sunlight conditions. Delayed harvest in AV did not increase the grain yield and the reduction were still between 20.3% to 22.8%. Reduction of grain yield was mostly ascribed to the lower head number. However, when the grain yield in AV was compared with average grain yield in the Chikusei area without AV, the reduction is less than 20%. Thus, it is acceptable under MAFF's guideline.

Simulation models generated a high correlation of determinant ( $R^2$ ) of 0.7873 (solar radiation model), 0.9832 for total biomass simulation (crop growth model), and 0.9873 (solar energy model). The high  $R^2$  indicated good fits of the model.

Scenario analysis concluded that the best tilt angle to gain optimum rice and energy production was at 25° in August. In contrast, the default tilt angle in August was at 14°. This finding provides a decision support to the farmer for considering changing the default tilt angle from 14° to 25° to gain slightly higher monetary benefit (0.06%) for both rice and energy production.

Findings from this research had shown modelling approaches (Revit & Dynamo, APSIM-Oryza, and PVSyst) are reliable and could provide robust estimates of solar radiation, rice yield, and energy production in AV. In conclusion, this study clearly advanced current knowledge from previous published studies that were not explicitly managed to find answer for the economically optimum conditions for rice yield and energy production.

# **Chapter 1: Introduction**

## **1.1 Agrivoltaic concept**

Agrivoltaic (AV) concept was first proposed by Goetzberger and Zastrow in 1982 by combining solar photovoltaic energy production with crops in open field condition. Solar photovoltaic panels are installed at about 2 meters above the ground and the space beneath the panels can be used for agriculture activity (Goetzberger & Zastrow, 1982). Agrivoltaic is the combination of two words, agriculture and photovoltaic. It was defined by Dupraz et al. (2011) as mixed systems associating solar photovoltaic panels and crop at the same time on the same land area. AV has attracted attention of farmers and energy investors because of the benefit to produce food, and in addition, power at the same time.

The need for new sources of renewable energies and the rising price of fossil fuels have induced the hope that energy crops (i.e. corn, sugarcane) may be a source of biomass energy for the future (Dupraz et al., 2011). Energy crop will therefore compete with food crop for land usage. It is a major constraint to the countries where land price is high and land availability is scarce. AV was an innovative solution to solve the competition of land around the year 2000s when many farmers in the US and Europe started to convert their land from food crops to energy crops due to higher demand of biofuel energy (Dixon et al., 2010). The expansion of AV may contribute to reconcile food security and green energy supply.

## **1.2 Agrivoltaic system in Japan**

Agrivoltaic system (AV) is also named as “solar sharing” in Japan. This concept was invented by Akira Nagashima in 2004 in Japan. He patented the stilt-mounted AV he designed and made the patent free for public use in 2005 (Nagashima, 2005). Nagashima’s design uses steel pipes as stilt without using concrete footing for easy dismantle. Rows of solar photovoltaic panels are mounted above the ground and arranged at certain intervals to allow enough sunlight to penetrate to the ground for photosynthesis of crops. This design allowed adequate sunlight for crops and sufficient space for agricultural machinery (Sekiyama and Nagashima, 2019).

While AV proved to be technically feasible and provides multiple benefits, the use of agricultural land to install solar photovoltaic has been constrained by Japan government to avoid competition with food production (Homma et al., 2016). In the past, the use of

agricultural land for applications other than agriculture has been prohibited in Japan by regulation by the farmland law. However, in 2013, part of the agricultural land law was revised which made it possible to use agricultural land for renewable energy production (MAFF, 2013). By revitalizing the agriculture law, government of Japan aimed to utilize the benefit of AV for creating effective utilization of agricultural land for renewable energy production.

At the same time, however the Ministry of Agriculture, Forestry and Fisheries (MAFF) restricted the use of AV by enacting a guideline related to AV. The condition of the guideline imposes that crop yield should not decrease more than 20% compared to the average same crop yield in the same area (MAFF, 2013). If the condition cannot be satisfied, the power generation facility would need to be removed.

### **1.3 Rice (*Oryza sativa*) the most important cereal crop in Japan**

Rice is the staple food for more than half of the world's population (Li et al., 2017). Worldwide total consumption continues to increase due to population growth and a rapid increase in rice consumption in many countries. Productivity therefore will have to increase to meet the growing demand and keep rice affordable.

In Japan, rice is also by far the most important crop. It was planted from the northernmost island in Hokkaido to the southernmost island in Kyushu (GRiSP, 2013). Rice remains important in the Japanese daily life and culture. In Japan, rice planting area is 1.6 million ha (4% of total land area in Japan). If AV is adopted on 1% of the acreage area of the rice farmland, this would be equivalent to total solar power capacity installed as of 2014 (Homma et al. 2016). The impact would be significant if many rice farmers adopt AV for their rice fields.

### **1.4 Energy demand in Japan**

Great East Japan Earthquake in 2011 had drastically changed Japan's energy policy and lead to a greater focus on renewable energy. Many nuclear plants had been shut down due to the fear of future accident caused by the earthquake. Government of Japan is targeting to reduce the dependency of nuclear power generation by introducing renewable energy sources such as solar, wind, geothermal, hydro and biomass.

Today, Japan is on the way of reshaping strategies of energy production and decreed that by 2020, 20% of the energy must come from renewable sources which should become at least 27% by 2030 (Hirata, 2014). In 2018, the share of total renewable energy generation in Japan had increased to approximately 17.4% from 16.4% in 2017 (ISEP, 2018). The amount of solar photovoltaic generation had also increased from 5.7% in the 2017 to 6.5% in 2018. This is very close meeting the target value of the 5th Basic Energy Plan implemented by government of Japan and hope to achieve at least 27% of renewable sources by 2030 (METI, 2018).

### **1.5 Feed-in Tariff scheme in Japan**

Feed-in Tariff (FIT) scheme was first introduced in Japan in July 2012 to encourage the use of renewable energy sources. This scheme made mandatory for electric utility operator to buy electricity from renewable sources at fixed prices for 10 to 20 years depending on the installed capacity (Kimura, 2017). At the same time, this scheme encouraged farmers to use their existing farmland to continue cultivate crops beneath the solar panels. AV provides farmers an opportunity to increase their income from selling electricity besides crops.

### **1.6 Agrivoltaic research around the world and in Japan**

Although AV has been theoretically established in the early 1980s, the first detailed AV farm experiments were performed in Montpellier France in 2010 (Dupraz et al., 2011). The research of Marrou et al. (2013) had analysed the behaviour of lettuce crop under shading of fixed solar photovoltaic panels. Solar photovoltaic panels in AV create intermittent shading and reduce the average available light for the crop. Marrou et al. (2013) found that light reduction was not necessarily detrimental for crop production. An experiment conducted for spring and summer lettuces in AV showed that lettuce yield was maintained despite shading (Marrou et al., 2013). It showed that lettuce, a sciophyte or shade (tolerant) plant could adapt its morphology (e.g. producing thinner and wider leaves) without yield reduction when it is grown under AV. In US, lettuces grown in the partial shade of photovoltaic panels indicated a gain of 30% increase in economic value gained from overall electricity coupled with lettuce production when compared to conventional agriculture (Dinesh & Pearce, 2016). A modelling analysis was performed to simulate plant production using STICS model ([https://www6.paca.inra.fr/stics\\_eng/](https://www6.paca.inra.fr/stics_eng/)) and energy production using PVSyst

(<https://www.pvsyst.com/>) to gauge the technical potential of scaling-up AV in US (Dinesh & Pearce, 2016). Tani et al. (2014) showed an improvement of lettuce growth by using light diffusion films under roof-mounted solar photovoltaic modules in the greenhouse. However, to obtain proper plant growth throughout the year, the shortage of light into the greenhouse during winter season may be problematic. Therefore, it is still crucial to increase daily irradiance at the low sun angle during wintertime. Another research was conducted on lettuce in France under AV but using mobile solar photovoltaic panels that tilt angle could be tilted to capture the daily irradiance. The result showed higher productivity per land area using mobile solar photovoltaic panels, while maintaining biomass production of lettuce close or even similar to full-sun condition. Lettuce is considered shade tolerant plant because lettuce performed adaptive capabilities to adjust to the shading caused by the solar photovoltaic panels (Valle et al., 2017). The studies reviewed above only indicate that AV is effective for the system with shade plant such as lettuce (Dinesh & Pearce, 2016). If AV are only applicable to commercially less viable shade-tolerant crops or vegetables, the system cannot be widely utilized.

However, the effectiveness of the system for heliophyte (shade plant or shade-intolerant plant), which are expected to grow less in low light environment, has not yet been explored sufficiently. Many major commercial crops, such as maize, rice, wheat, and vegetables such as tomato, cucumber, pumpkin, cabbage, turnip, are shade-intolerant and presumably require sufficient sunlight (Sekiyama & Nagashima, 2019). Sekiyama and Nagashima (2019) explored the performance of shade-intolerant crops. Their research showed that the maize yield under low density AV was higher than the control configuration by 4.9%. The results will encourage more conventional farmers, clean energy producers and policy makers to consider adopting AV, particularly in areas where land resources are relatively scarce (Sekiyama & Nagashima, 2019). However, the study area was only 100 m<sup>2</sup> and further research is required on a larger scale AV to reduce border effect. In addition, a study was also conducted in Italy on maize during summer season under water limited conditions (Amaducci et al., 2018). The result from simulation indicated higher and more stable grain yield under AV than under full light condition mainly due to the less water loss via evapotranspiration in AV.

## 1.7 Movable solar photovoltaic panels in AV research

In AV system, there are two types of arrangement in solar photovoltaic panels. The first type is fixed solar photovoltaic panel, i.e. panels' tilt angle is fixed at designated degree and could not be changed. Plants are cultivated under and between the solar photovoltaic panels (Figure 1.2). The second type of AV is movable solar photovoltaic panels either in single-axis or dual-axis. The single-axis system is aligned to north-south or east-west. While the dual-axis system is aligned in two directions, north-south and east-west to capture maximum of sunlight. In this experiment, movable solar photovoltaic panels with single-axis direction aligned to north-south is selected (Figure 1.2). This system can reduce shading in plant by adjusting the tilt angle at different growth stages.



**Figure 1.1 Fixed solar photovoltaic panels in AV system.**



**Figure 1.2 Movable solar photovoltaic panels in AV system (Source: <https://solar-sharing-japan.blogspot.com/2014/>).**

## **1.8 Selection of rice in AV research**

In this research, rice was selected for the experiment. The reason of choosing rice is due to the large potential of multiplier effect. In Japan, rice planting area is 1.6 million ha, which is about 4% of total land in Japan. If AV can be applied on existing rice fields, the potential of increasing solar power generation is very large. In addition, rice is the main staple food in Japan, and so continuing rice cultivation is very important to maintain food security, farmers' livelihood and flood control.

Homma et al., (2016) conducted a field experiment in a paddy field with fixed AV in Chiba prefecture, Japan. The solar panels were tilted at 30° and horizontal projection of solar panels area on ground is 34%. The rice cultivar used in this field experiment was Koshihikari. Under the shading condition, heading time was delayed significantly. Number of panicle and weight per panicle was significantly less compared to open field condition. By utilizing measured data from the experimental field, the study modified the conventional crop model to simulates rice yield under the shade of solar photovoltaic panels. The study indicated a 20% shading from solar photovoltaic panels reduces the rice yield by approximately 20% (Homma et al., 2016).

## **1.9 Relationship between solar radiation and rice yield**

Rice plant normally takes 100-160 days from germination to ripening, depending on the variety and the environment under which it is grown. Within this growing period, the life of rice plant can be categorized into three growth phases, ie.,vegetative, reproductive and ripening stages (Vergara & Chang, 1985). The vegetative growth phase can be further divided into basic vegetative phase (BVP) or juvenile stage and the photoperiod-sensitive phase (PSP). The former growth stage of plant is not affected by photoperiod (Vergara & Chang, 1985).

Numerous studies had indicated the significant and positive correlation between solar radiation and rice grain yield. In a ten years field experiment conducted from 1968 to 1977 at IRRI, solar radiation at various stages of rice growth was correlated with grain yield. Yields of all four varieties (IR5, IR8, H-4, Milfor) were most significantly correlated with solar radiation during reproductive and the ripening stages (Evans & De Datta, 1979). High solar radiation at any stage after panicle initiation was associated with high yield in both older and modern rice varieties (Evans & De Datta, 1979). In another field experiment conducted at Los Banos, Philippines, grain yield for an improved early maturing variety showed highly positively

correlated with average daily solar radiation and negatively with average daily mean temperature, during the reproductive stage (i.e. the 25-day before flowering) (Yoshida et al. 1976). However, variation in solar radiation and temperature during the vegetative stage do not have any overall effect on yield and yield components. A field experiment conducted in Bangladesh Rice Research Institute also showed a linear relationship between solar radiation and grain yield during reproductive and ripening stages.

To avoid rice yield decrease more than 20% as per MAFF’s guideline, finding critical period for sunlight requirement is very important. The tilt angle of solar panels can be adjusted to allow more solar radiation reaching plant canopy during the critical period to increase rice yield. A research on the effective utilization of sunlight conducted in Texas summarized critical period for sunlight throughout the rice growing stages (Stansel, 1975; Nyang’Au, 2014). They reported that the critical period started from panicle initiation to medium dough stages. Within this period, first heading stage required the highest cumulative sunlight (Figure 1.3).

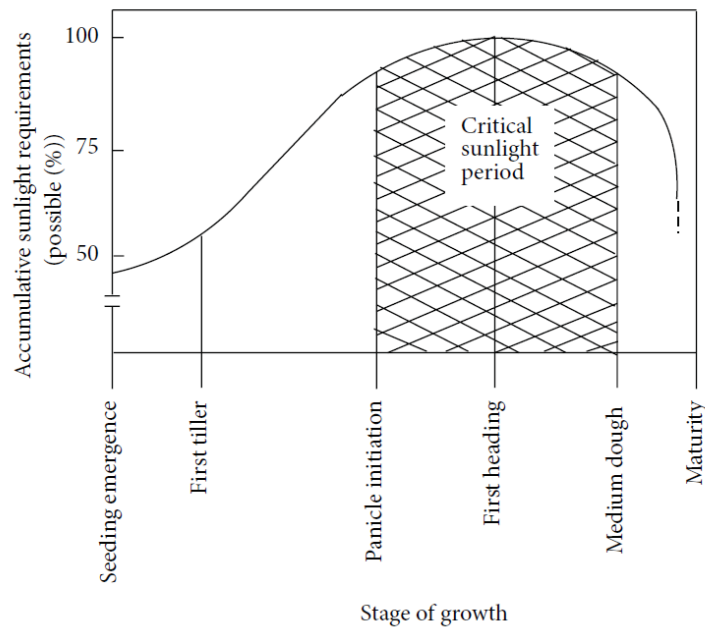


**Figure 1.3 Solar radiation requirement of rice at different stages of growth and development (adapted from Stansel, 1975).**

### **1.10 Research objective**

Throughout the literature review up to date, it is understood that accumulation of empirical research about movable solar photovoltaic panels in AV is very limited in Japan. Although there are numerous researches examples on the influence of insufficient solar radiation on the crop growth, field experiment and modelling study are still lacking. There are only limited studies examined the influence of partial shading from fixed solar photovoltaic panels on the rice in Japan. Most of the previous studies in AV were focused on lettuce, tomato, cucumber, and maize. Thus, this bring to the research objectives as below:

1. To estimate the effect of rice yield under partial shading condition of movable solar photovoltaic panels in AV system.
2. To establish the methodology of using crop growth model through calibration and validation by using field experimental data.
3. To establish the methodology of using light distribution model and solar energy model.
4. To optimize the solar photovoltaic panels' tilt angle by finding economically optimum rice and energy production through scenario analysis.

## **Chapter 2: Effect of partial shading on rice grain yield and energy output**

### **2.1 Introduction**

The deployment of agrivoltaic system in the rice field is getting popular in Japan. However, the effect of partial shading from movable solar photovoltaic panels on the rice grain yield are not widely known. The purpose of this chapter was to investigate the effect of partial shading from movable solar photovoltaic panels on rice by conducting experiment in agrivoltaic system in a farmer's field. Energy generated from the solar photovoltaic system was also collected for analysis.

### **2.2 Materials and methods**

#### **2.2.1 Site description**

A field experiment was conducted at a field of rice farmer (36°19'7.06"N, 139°55'42.60"E) at Chikusei, Ibaraki Prefecture, Japan. Agrivoltaic system was installed at a part of the paddy field in March 2016 by the farmer and the field experiment of this study was conducted in summer in 2018. Soil taxonomy order is Entisols and suborder is Fluvents as classified by USDA (SoilGrids, 2019). It was classified as Haplic Fluvisols by FAO soil classification (SoilGrids, 2019).

#### **2.2.2 Experimental plot**

The total plot area was 4,002m<sup>2</sup> and a part of the field (1,415m<sup>2</sup>) on which the panels were installed was designated as AV (agrivoltaic system, i.e., the combination of solar panels and the part of rice field under the solar panels) and the remaining part of the plot (2,587m<sup>2</sup>) was as OP (open area, area not covered by solar panels). Depending on the angle of the radiation, the margin area of rice field in AV received direct solar radiation particularly in the morning and evening. On the other hand, the solar panels and their supporting structure shed shadow to a part of OP near the solar panel.

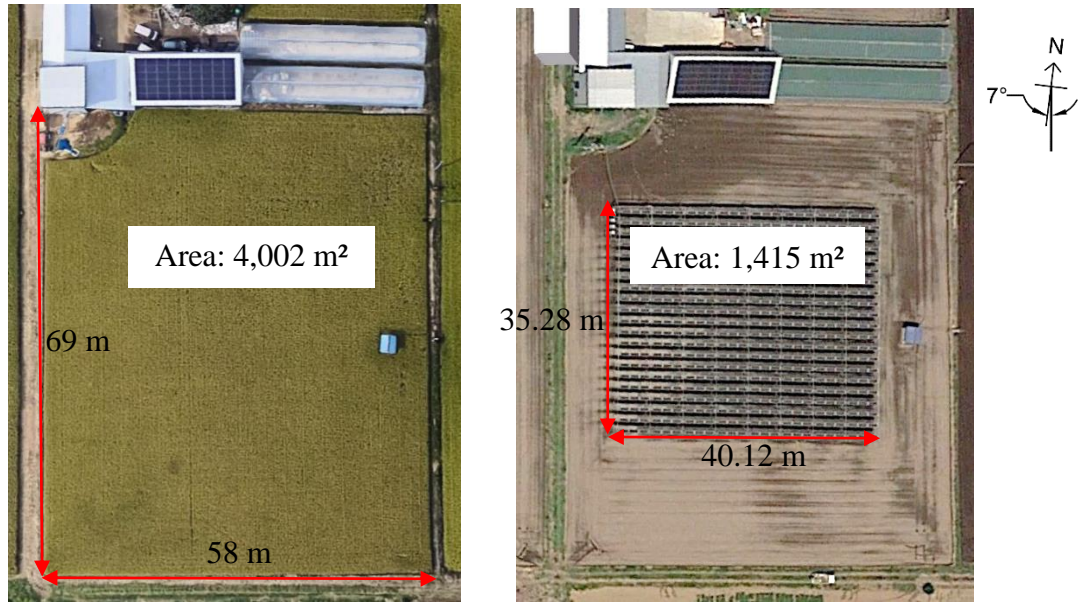


**Figure 2.1 Experimental plot in Chikusei city, Ibaraki prefecture. Left: before agrivoltaic system installation, and right: after the installation of agrivoltaic system. (Google earth, downloaded on 1 April 2019)**

The solar photovoltaic panel part of AV was made of the combination of modular structures. There were seven rows and eight columns of solar panels. Each modular structure was 5.015 m (length) and 5.04 m (width). Figure 2.2 shows schematic layout of AV and sensors locations in the field. Total size AV plot was 35.28 m (north-south direction) and 40.12 m (east-west direction). Height of the modular structure was 3.5 m (Figure 2.3) from ground to allow movement of machineries such as rotary tiller, mechanical transplanter, and combine harvester. Each modular structure consisted of 9 units of solar panels. The size of each solar panel was 1.482 m (length) by 0.515 m (width) and panel area is 0.7632 m<sup>2</sup> per unit. A total of 504 units of solar panels were installed on the steel structure and equivalent to 384.65 m<sup>2</sup>. Horizontal ground projection calculated by dividing total solar panels area by AV plot area was 27.18%. This is used as a reference value of shading under solar panels. In other words, solar panels created 27.18% shading on the rice crop. Solar panels were facing to the south with slightly twisted to the east (7°). The solar panels tilt was changed manually to the predetermined angle for each month (Table 2.1) to capture maximum solar radiation for energy generation.

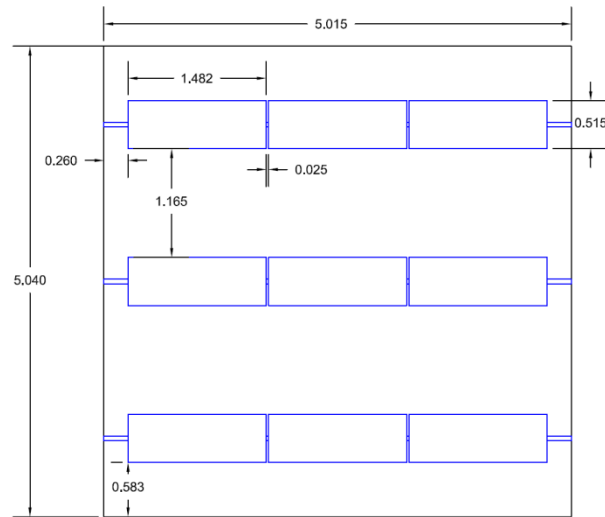
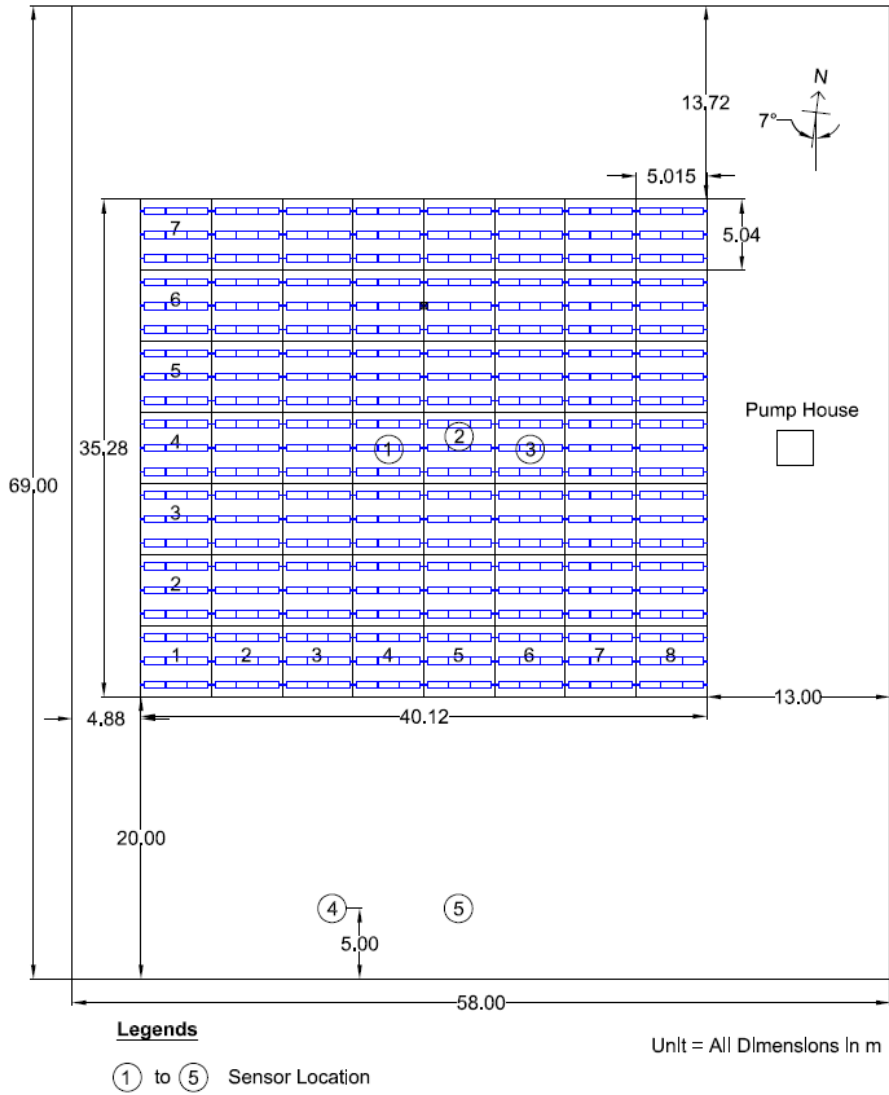


**Figure 2.2 Schematic layout of agrivoltaic system with environmental sensors (top) and modular structure (bottom).**

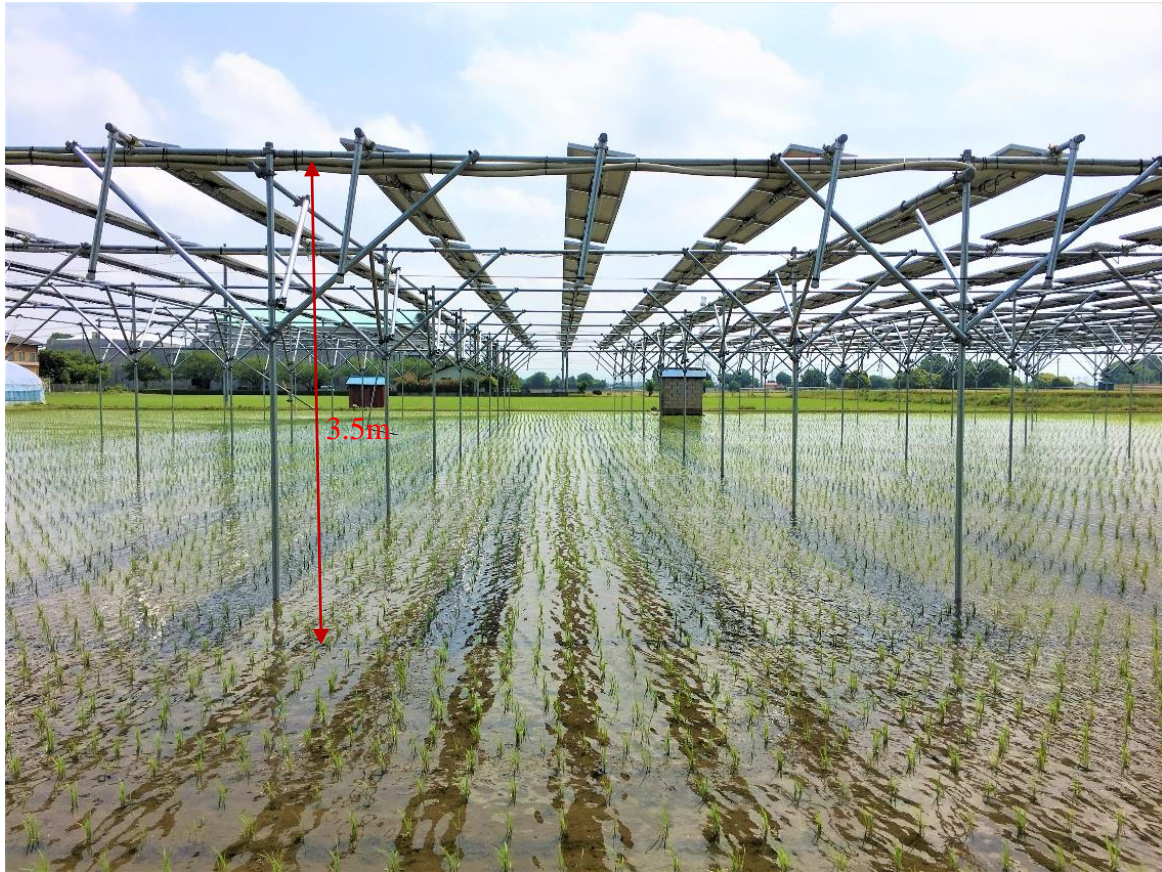


**Figure 2.3 Agrivoltaic system tilted at 10° (taken on 25 May 2018)**

**Table 2.1 Solar panels tilt angle**

Month	Jan	Feb	Mar	Apr	May	June	July	Aug	Sept	Oct	Nov	Dec
<b>Tilt Angle (°)</b>	60	51	36	20	10	10	10	14	25	42	55	60

### 2.2.3 Crop management

Rice cultivar Asahi-no-yume was used for the experiment. This cultivar was developed in Aichi prefecture, and was registered in 1996. It was adopted in 2000 as recommended variety in Tochigi prefecture, and was also adopted as recommended variety in Tomo area of Gunma prefecture in 1999 to replace rice cultivar Goropikari. And later it was introduced in Chikusei area in Ibaraki prefecture. Asahi-no-yume is better in resistance to diseases and insects with high yielding ability compared to Goropikari but is a late maturing (Takahashi & Yoshida, 2007).

Seeds were soaked in the water for 5 five days at the water temperature of 15 °C. Then, water temperature was increased to 32 °C for 24 hours before sowing. Good and germinated seeds were selected for sowing. Sowing was conducted on 16 April 2018. Seeds were sown in the nursery box, each size at 30 cm x 60 cm and kept in the vinyl greenhouse. Seedlings were watered twice a day at 10:00 and 15:00 to ensure enough soil moisture during the nursery stage. Twenty-five days-old seedlings were transplanted by transplanter at 2-5 seedlings per hill on 11 May 2018. Planting densities were 60 hills per 3.3 m<sup>2</sup> and equivalent to 18.18 hills m<sup>-2</sup>. Row spacing was 30 cm while between-hill spacing was 18.33 cm (Figure 2.5). Compound fertilizer containing 15% N, 10% P<sub>2</sub>O<sub>5</sub>, 10% K<sub>2</sub>O was used and applied as basal fertilizer (48 kg N ha<sup>-1</sup>, 32 kg P<sub>2</sub>O<sub>5</sub> ha<sup>-1</sup>, and 32 kg K<sub>2</sub>O ha<sup>-1</sup>) after puddling and prior to transplanting. Additional fertilizer in capsule form (12 kg N ha<sup>-1</sup> and 8 kg K<sub>2</sub>O ha<sup>-1</sup>) was applied as top dressing which will break down at the end of July 2018 during the highest temperature period within the growing season. Same fertilizer rate was applied in both AV and OP plots. Water level was maintained at 5 to 6 cm during transplanting and increased to 10 to 15 cm one month after transplanting. Water was drained one week before harvesting to ease operation of combiner harvester. Harvesting was conducted at OP on 6 October 2018 (148 days after transplanting (DAT)). Delayed harvests were carried out four days after, harvesting on 10 October 2018 and eleven days after, harvesting on 17 October 2018 at AV. Table 2.2 summarizes crop phenology events.

**Table 2.2 Crop phenology events**

Phenology	Sowing	Transplanting	Heading	Harvest	Delayed Harvest	
	Date	11/May	17/Aug	06/Oct	10/Oct	17/Oct
Days after transplanting (DAT)	-	0 (25 DAS)	98	148	152	159
Location				AV, OP,	AV	AV
Sampling number				AV (s1, s2, s3) OP (s4, s5, s6)	s7, s8, s9	s10, s11, s12

Note: DAS = Day after sowing. OP = Open area plot, AV = Agrivoltaic system plot.

#### 2.2.4 Weather measurement

A set of sensors consisted of a solar radiation and temperature sensors were installed in the AV and OP plots (Figure 2.2) from the reproductive phase (2 August 2018) to the ripening phase (5 October 2018). Three sets of the sensors were installed in the middle of AV (sensor 1 to 3). Among them, sensor 1 and 3 were installed directly under solar panels while sensor 2 was between solar panels. Two sets of the sensors (sensor 4 and 5) were installed at the southern part of OP plot, at the position 5 m away from the southern edge of the solar system. Solar radiation and air temperature at crop canopy level were measured at every ten minutes in each plot. Silicon pyranometer (ML-01 – Environment Measurement Japan Co. Ltd., Japan) and temperature sensor (MIJ-LTP – Environment Measurement Japan Co. Ltd., Japan) were connected to datalogger (MIJ-01 – Environment Measurement Japan Co. Ltd., Japan) and installed in the AV plot (Figure 2.4a).

In the OP plot, silicon pyranometer (SP-110-SS – Apogee Instruments Inc., USA) and temperature sensor (RT-1 – Meter Group Inc., USA) were connected to datalogger (Em50 – Meter Group Inc., USA) (Figure 2.4b). In addition, solar radiation sensor (SPM-SD – Sato Shouji Inc., Japan) and temperature sensor (TM-947SDJ – Sato Shouji Inc., Japan) were also installed in the OP plot. All the sensors were calibrated prior to the measurement.

Temperature and solar radiation data were also collected at the experimental field from 2 August to 5 October 2018 (one day before harvest) (Figure 2.10 and Figure 2.11). In the AV plot, solar radiation data were collected from two locations, directly under the solar panel (AV Rad-Under) and between solar panels (AV Rad-Betw). In the OP plot, solar radiation data were taken 5 m distance from the edge of the experimental field which is free from any shading and obstruction object. Temperature data were taken at the same location with solar radiation.

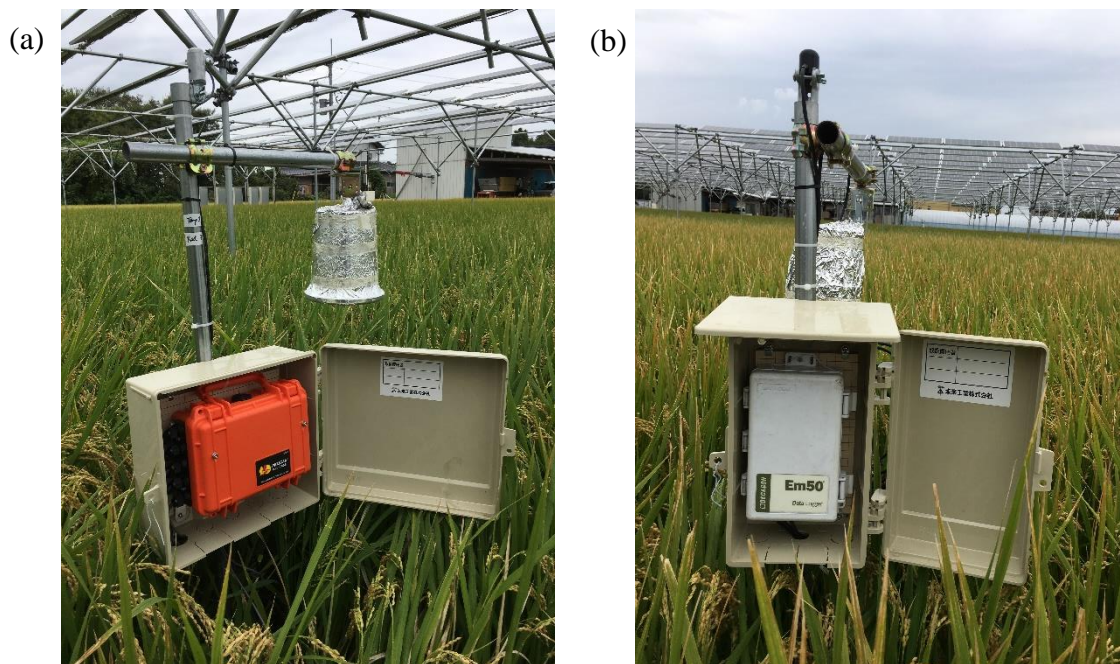


**Figure 2.4 (a) Sensors and dataloggers in AV plot. (b) Sensors and dataloggers in OP plot.**

Daily precipitation, maximum and minimum temperature were collected from Japan Meteorological Agency (JMA) Shimodate weather station. Solar radiation data were collected from JMA Tsukuba weather station since the data was not available at Shimodate weather station. Shimodate weather station is 9.1 km while Tsukuba weather station is 41.5 km away from the experimental field. These two weather stations are the nearest weather station to the experimental field.

### 2.2.5 Plant growth measurement

Plant growth stages were monitored at heading and harvest by the farmer. Heading date was determined as three days before flowering date. Flowering date was determined as when 50% of plants were flowering in the field.

Total six times of plant samplings were conducted throughout the rice growing season (Table 2.3). First three samplings were collected at the different rice growing stages while last three samplings were collected at the maturity stage. In the AV plot, delayed harvest was conducted to determine the effect of after-ripening on grain yield according to the suggestion of the farmer. At each sampling, two hills with three replications were collected in both AV

and OP plots. Plant samples were collected for biomass measurement. After measuring fresh weight, plants were separated into leaves, stem, and panicle, and dried in an oven at 70 °C for 72 hours, and dry weight was measured.

Samplings at harvest were collected from three locations in AV plot (s1, s2, and s3) and in OP plot (s4, s5, and s6). Delayed harvest samplings in AV plot were collected on 10 October 2018 (s7, s8, and s9) and on 17 October 2018 (s10, s11, and s12) (Figure 2.5). Sampling size in AV and OP plots were 16 hills and 15 hills respectively (Figure 2.6). Each sampling area for AV was 0.88 m<sup>2</sup> while that for OP was 0.82 m<sup>2</sup>. Sampled plants were kept in vinyl greenhouse to allow natural drying about two weeks. Then, plants were separated into straw and grain by threshing machine. The threshed grain went through winnowing process to remove the debris. After that, dry weight was measured.

**Table 2.3 Sampling information**

Date	DAT	Sampling Purpose	Sampling Area and Location*	
			AV Plot (m <sup>2</sup> )	OP Plot (m <sup>2</sup> )
23/6/2018	43			0.11
1/8/2018	82	Plant Growth		0.11
6/9/2018	118			0.11
6/10/2018	148	Harvest	0.88	0.82
10/10/2018	152	Delayed Harvest	0.88	-
17/10/2018	159		0.88	-

\* Each sampling with three replications

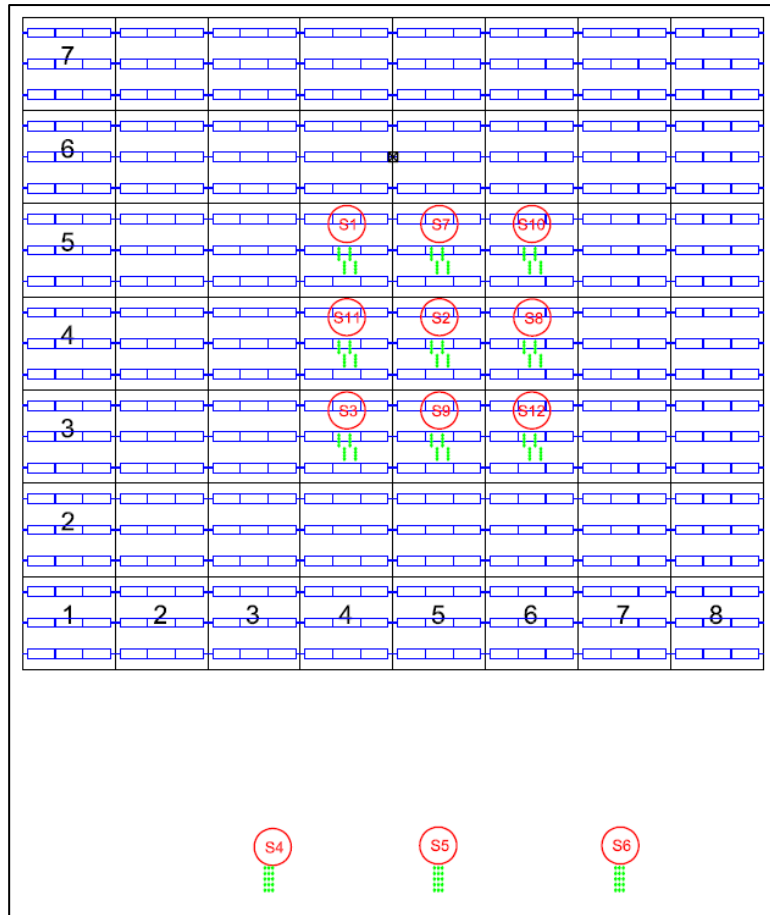


**Figure 2.5 Sampling locations at harvest (s1 to s6) and delayed harvest (s7 to s12).**

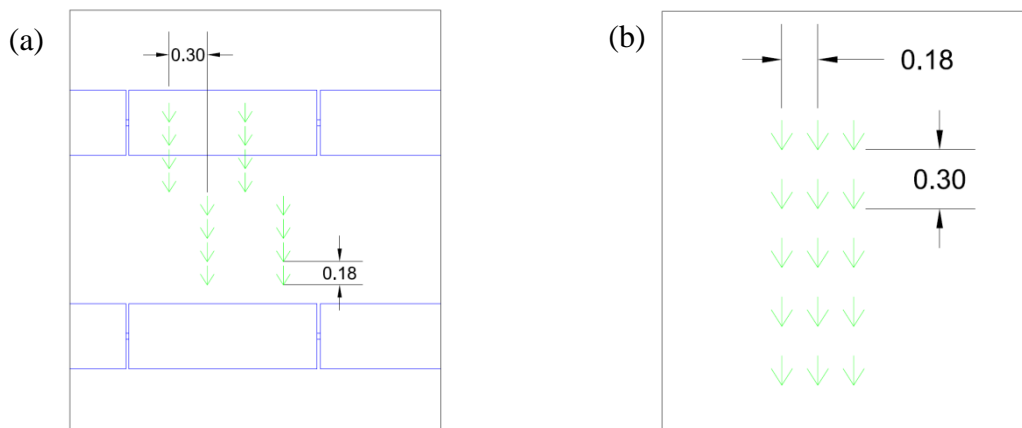


**Figure 2.6 a) Sampling in AV plot and b) Sampling in OP plot.**

#### 2.2.5.1 Leaf area index (LAI) measurement

Leaf area index (LAI) were measured twice during the rice growing season. First measurement was done on 1 August 2018 (82 DAT) and second measurement on 6 September 2018 (118 DAT), same date as the plant growth sampling. Two plant samples for LAI measurement were collected, one for AV plot and another for OP plot. Plants were separated into leaves, stem, and panicle. Leaf area was measured by Leafscan app (<http://www.leafscanapp.com/>). Firstly, to determine the scale and correct perspective of the leaf, four “reference markers” were used. Length of the reference marker was set as 10 cm in the Leafscan app. Secondly, reference markers from the Leafscan user guide was printed on an A4 white paper. The length between the reference markers was checked to ensure 10 cm between rows and columns. Next, leaf was cut into two or three parts (depends on the leaf length) and placed entire leaf within the reference markers on A4 paper. Then, leaf was flatten using a transparent file folder. Finally, leaf area was measured by adjusted the saturation threshold and taking photo. The leaf area was measured continuously and stop until approximately 500 cm<sup>2</sup>. Leaf area data was transferred to csv file for recording purposes.

The measured leaves were dried in an oven at 70 °C for 72 hours, and dry weight was measured. Specified leaf area (cm<sup>2</sup>/g) was calculated by divided measured leaves area by leaves dry weight. Leaf area index was calculated multiplying specified leaf area with measured leaves dry weight.

#### 2.2.5.2 SPAD measurement

SPAD values were taken on weekly from August to September by using Chlorophyll Meter (SPAD-502, Konica Minolta). Total eight times of SPAD value had been recorded. Five plant samples continuously at the same row at the medium growth location was selected. Average reading of three leaves were taken from full grown leaves. SPAD value were taken in each AP plot and OP plot with three duplications.

#### 2.2.5.3 Culm length, head length, and head number measurements

Five plant samples continuously at the same row were selected from the medium growth location. Measurements were carried out for AV and OP plots at harvest and delayed harvest with three duplications. The longest culm length and head length were measured by using measuring tape. Total head number was counted manually from the plant samples.

#### 2.2.6 Combine plot yield

Interview with rice farmer was conducted on 15 April 2019 to obtain information of combine plot yield at the experimental site. Combine plot yield in AV and OP plots for year 2017 and 2018 were recorded. Average rice yield in Chikusei area for year 2017 and 2018 were also gathered through the interview.

#### 2.2.7 Solar photovoltaic system

Solar photovoltaic system consisted of 504 units of solar panels (LX-115M, Luxor Solar) and 5 units of inverters (EPC-S99MP5-L, EneTelus, Tabuchi Electric) (Figure 2.7). Table 2.4 summarises solar photovoltaic configuration. Solar panels received solar radiation to generate direct current. Direct current was converted to alternating current through inverters. Solar energy generated from the photovoltaic system were recorded in the datalogger on each day. Daily and monthly energy data were collected for validation purpose.

**Table 2.4 Solar Photovoltaic System Configuration**

<b>Inverter No.</b>	<b>No. of Solar Panel (unit)</b>	<b>No. of String</b>	<b>Total No. of Solar Panel (unit)</b>	<b>Total Solar Panel Capacity (kWp)</b>
1-4	20	5	100	$100 \times 115\text{Wp} \times 4 = 46.0$
5	20	1	20	$20 \times 115\text{Wp} = 2.30$
	21	4	84	$84 \times 115\text{Wp} = 9.66$
	Total	25	504	57.96



**Figure 2.7 Solar Panels and Inverters**

## 2.3 Results

### 2.3.1 Weather conditions

Annual precipitation recorded from JMA Tsukuba weather station was 1149 mm in 2018 (Figure 2.8). The daily maximum temperature recorded 37.7°C (24 August 2018) at its highest, and the lowest daily minimum was -9.6°C (28 January 2018). Average daily solar radiation was 14.19 MJ m<sup>-2</sup> day<sup>-1</sup> in 2018 (Figure 2.9). The precipitation during the growing season from early April to mid of October was 864mm while highest maximum daily temperature and lowest minimum daily temperature were 37.7°C (24 August 2018) and 2.1°C (7 April 2018), respectively. The average daily solar radiation throughout the growing season was 16.84 MJ m<sup>-2</sup> day<sup>-1</sup> and it was 18.7% higher than the entire year in 2018.

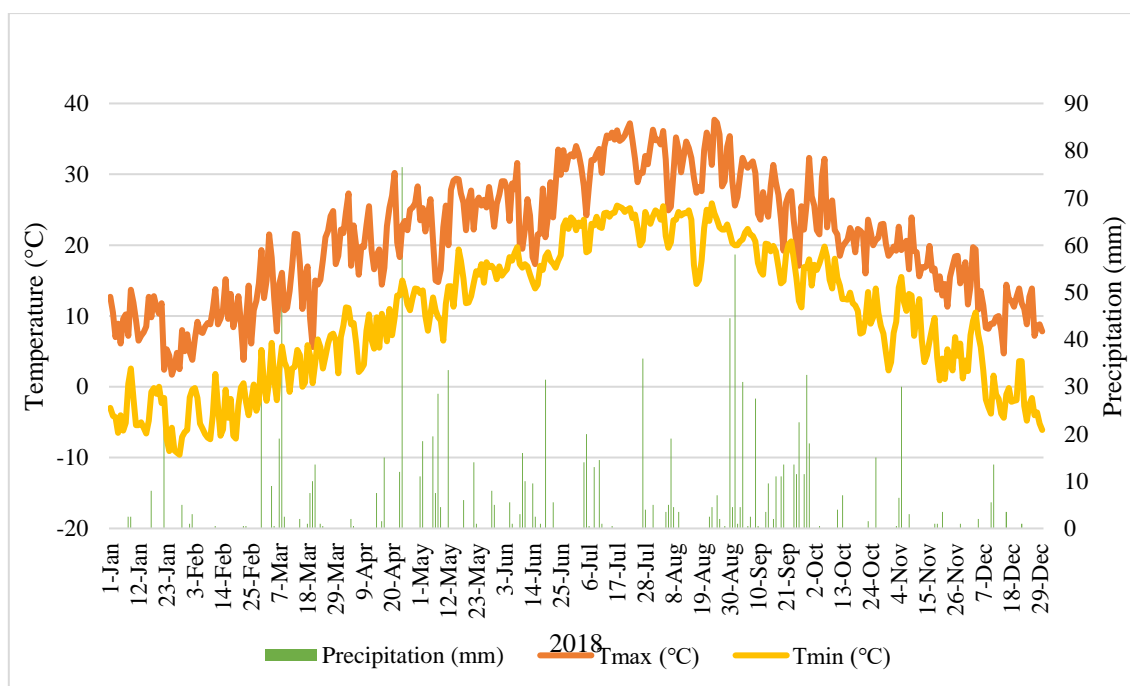


**Figure 2.8 Precipitation, maximum and minimum temperature collected from JMA Shimodate Weather Station.**

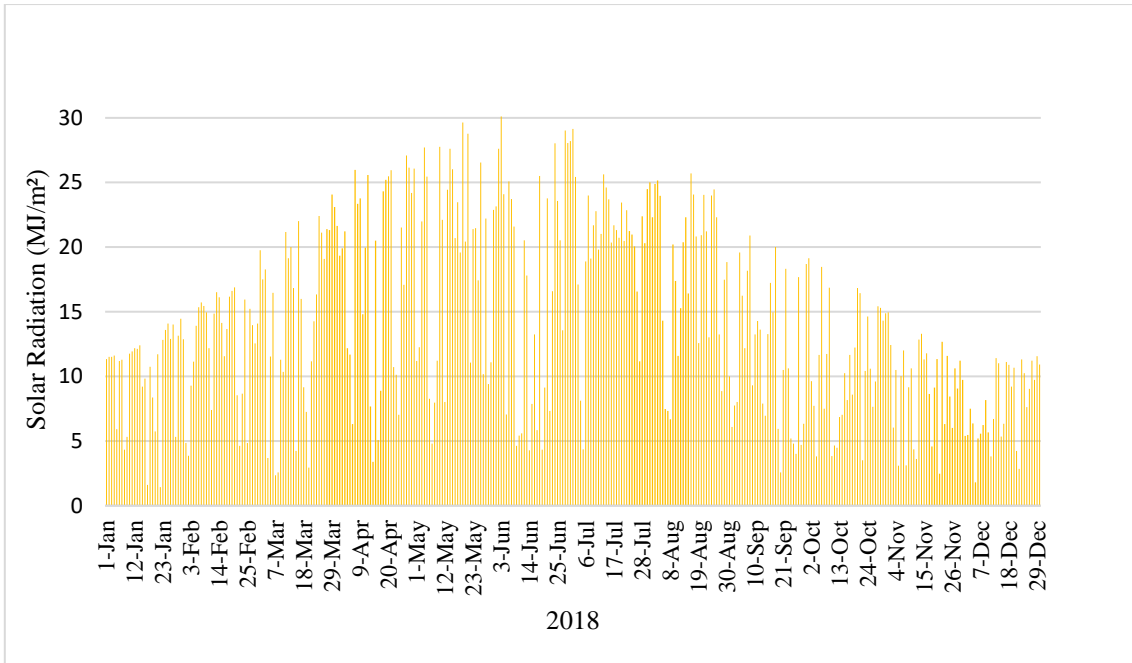


**Figure 2.9 Solar radiation collected from JMA Tsukuba Weather Station.**

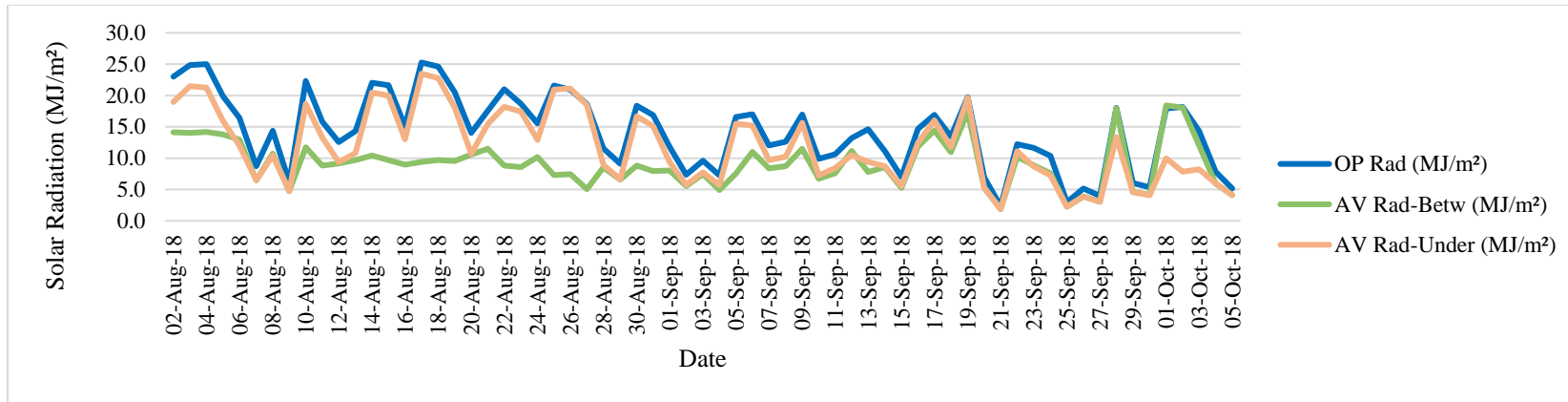


**Figure 2.10 Solar radiation collected from experimental field.**

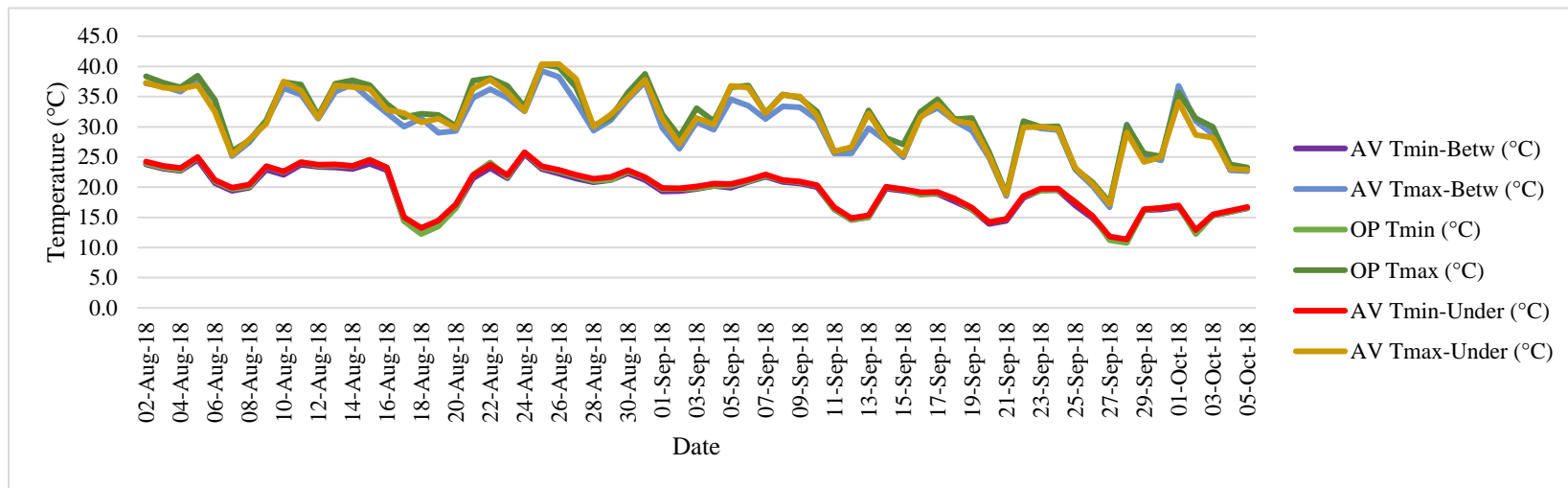


**Figure 2.11 Maximum and minimum temperature collected from experimental field.**

### 2.3.2 Dry matter production, leaf area index (LAI) and SPAD value

Leaf area index (LAI) were measured at 82 DAT (1 August 2018) and 118 DAT (6 September 2018). AV plot has slightly higher LAI than OP plot at 82 DAT. This is an indication of plant adaptation to lower solar radiation due to partial shading from solar photovoltaic panels in AV. However, LAI at OP plot was much higher than AV plot at 118 DAT (Figure 2.12: Leaf Area Index (LAI)Figure 2.12). At the maturity stage, plant was not able to sustain leaf growth and have lower leaf area. And generally, SPAD value at AV plot was higher than that at OP plot (Figure 2.13). From the field observation, the leaves in AP plot were more greenish than OP plot. In addition, three times of sampling during the plant growing stages were conducted and total biomass was calculated. OP plot consistently showed higher total biomass than AV plot (Figure 2.14).

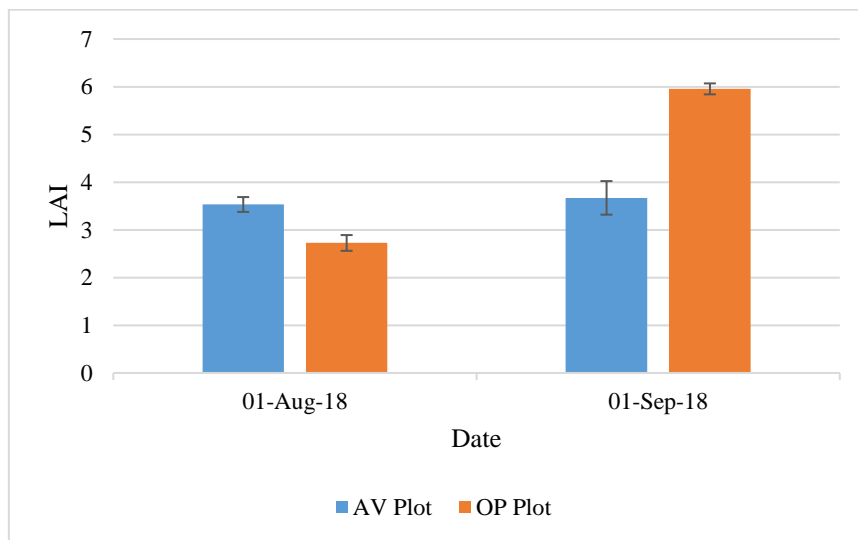


**Figure 2.12: Leaf Area Index (LAI)**

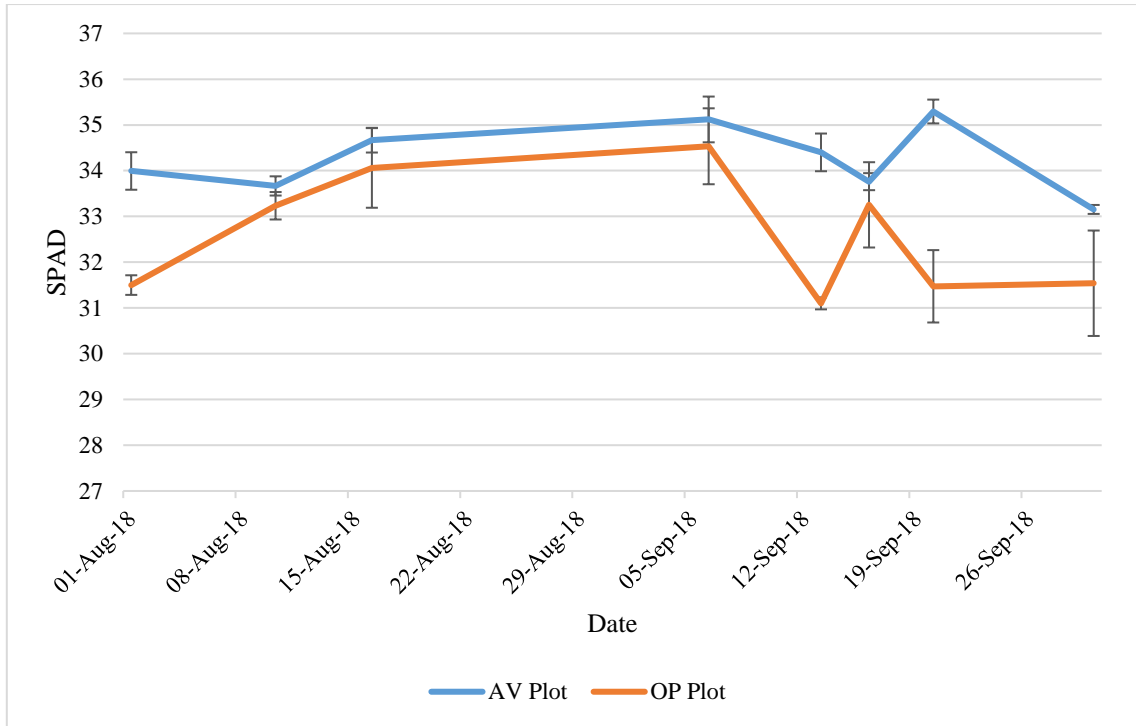


**Figure 2.13 Changes of SPAD values during rice growth**

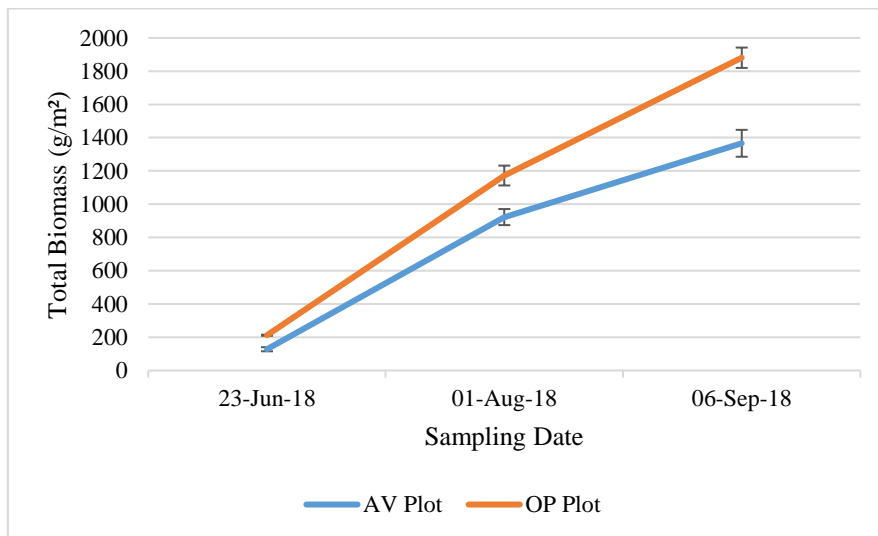
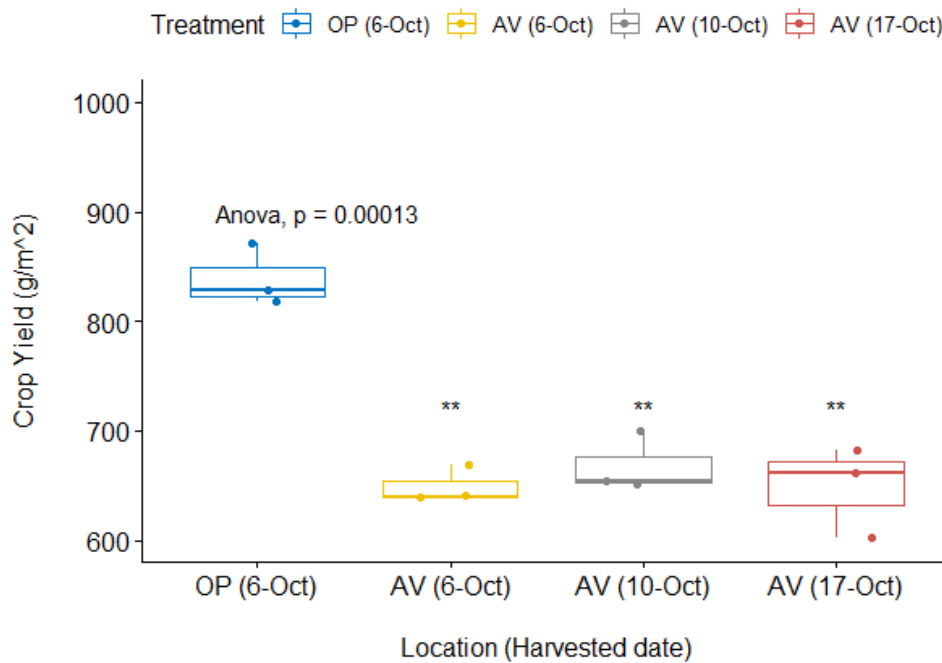


**Figure 2.14 Total biomass at different sampling date.**

### 2.3.3 Grain yield and total biomass

Grain yield was higher in OP plot than in AV plot of three harvesting periods (Figure 2.15 and Table 2.5). The grain yield in AV plot ( $649 \text{ g/m}^2$ ) was 22.6% lower than that in OP plot ( $839 \text{ g/m}^2$ ) on 6 October. On 10 October (4 days after normal harvest), grain yield in AV plot slightly (not significantly) increased to  $668 \text{ g/m}^2$  but maintained at  $648 \text{ g/m}^2$  at 17 October. Total biomass showed similar trend as grain yield (Figure 2.16). Harvest index (HI) was almost the same in AV and OP plots regardless of harvesting periods (Figure 2.17). HI were between 0.42 to 0.43 in all the plots.



(\*\* Significant at  $P < 0.05$ , Tukey's HSD test)

**Figure 2.15 Grain yield at different harvest dates.**

**Table 2.5 Grain yield and percentage difference.**

Date	Location	Grain Yield (g/m <sup>2</sup> )	Difference with OP (%)	Difference with AV on 6-Oct (%)
06-Oct-18	OP	839		
06-Oct-18	AV	649	-22.6	
10-Oct-18	AV	668	-20.3	2.9
17-Oct-18	AV	648	-22.8	-0.19

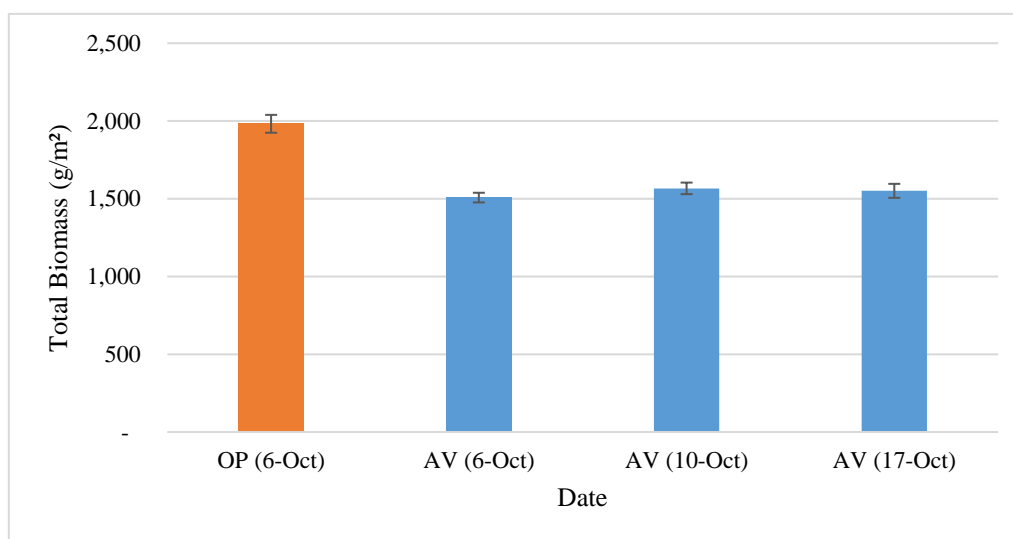


**Figure 2.16 Total biomass at harvest.**

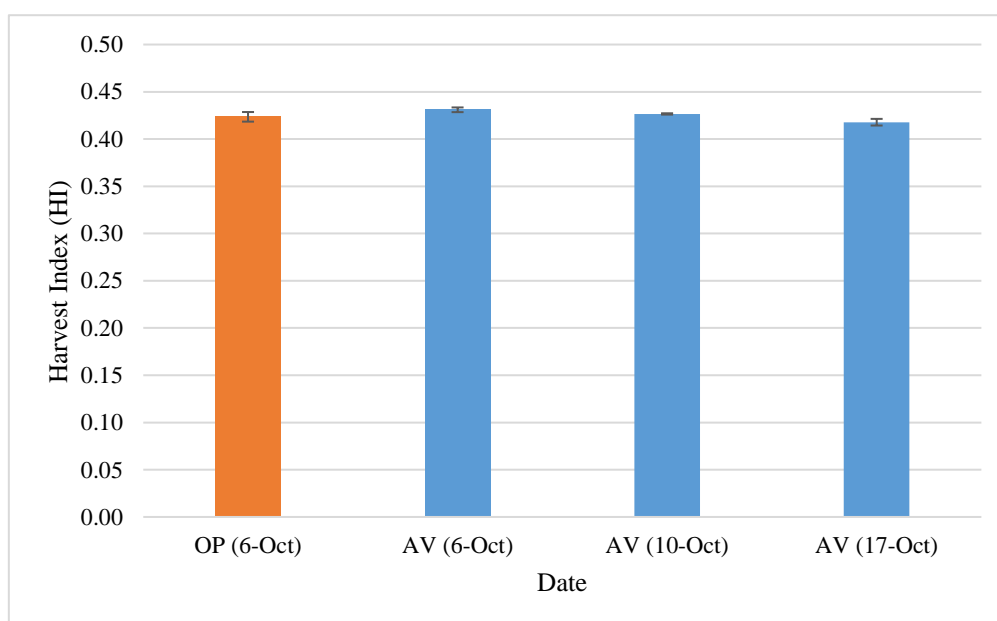


**Figure 2.17 Harvest index.**

### 2.3.4 Combine plot yield

Data provided from farmer on an interview carried out on 15 April 2019 indicated the actual rice yield in AV plot was at 5.29 t/ha (2018) and 5.10 t/ha (2017). In comparison with other rice farmers in Chikusei area, their average rice yield was 5.37 t/ha (2018) and 5.38 t/ha (2017). As a result, the reduction percentage of rice yield in AV plot compared to average rice yield in Chikusei area were very minimal at 1.4% (2018) and 5.2% (2017) (Table 2.6). This clearly indicated the rice reduction in AV could be less than 20% if farmers perform a good cultivation management and thus AV could fulfil the guideline enacted by MAFF (2013).

**Table 2.6 Comparison of combine plot yield in AV and average rice yield in Chikusei area**

<b>Year</b>	<b>Combine Plot Yield in AV (t/ha)</b>	<b>Average Rice Yield in Chikusei Area (t/ha)</b>	<b>Difference (%)</b>
2018	5.29	5.37	1.4
2017	5.10	5.38	5.2

(Note: Data provided by farmer on 15 April 2019)

A comparison in between the average rice yield in Chikusei area with experiment in OP plot demonstrated the same result. Experiment field in OP plot has higher rice yield at 6.2 t/ha (2018) and 6.5 t/ha (2017) (Table 2.7). This indicates the experiment field has a good management practices and produced higher rice yield than average yield in Chikusei area.

**Table 2.7 Comparison of average rice yield in Chikusei area and combine plot yield in OP**

<b>Year</b>	<b>Average Rice Yield in Chikusei Area (t/ha)</b>	<b>Combine Plot Yield in OP (t/ha)</b>	<b>Difference (%)</b>
2018	5.37	6.20	13.4
2017	5.38	6.50	17.2.

(Note: Data provided by farmer on 15 April 2019)

### 2.3.5 Culm length, head length and head number

Culm length and head length were consistently lower in OP plot than in AV plot. The culm length in OP plot (82.22 cm) and AV plot (91.83 cm) were recorded on 6 October (normal harvest). The highest head number was recorded in OP plot at 26.67 on 6 October.

**Table 2.8 Culm length, head length and head number at harvest**

Date	Location	Culm Length (cm)	Head Length (cm)	Head Number	Difference in Head Number (%)
06-Oct-18	OP	82.22	19.21	26.67	
06-Oct-18	AV	91.83	21.06	21.92	-17.8
10-Oct-18	AV	90.17	21.39	19.58	-26.6
17-Oct-18	AV	91.83	20.91	22.25	-16.6

### 2.3.6 Energy output from solar photovoltaic system

Highest energy output from solar photovoltaic system was in January (7,692 kWh) and second in July (7,584 kWh) due to more sunny days. Lowest energy output was in September (4,526 kWh) due to more raining days and typhoon effect.

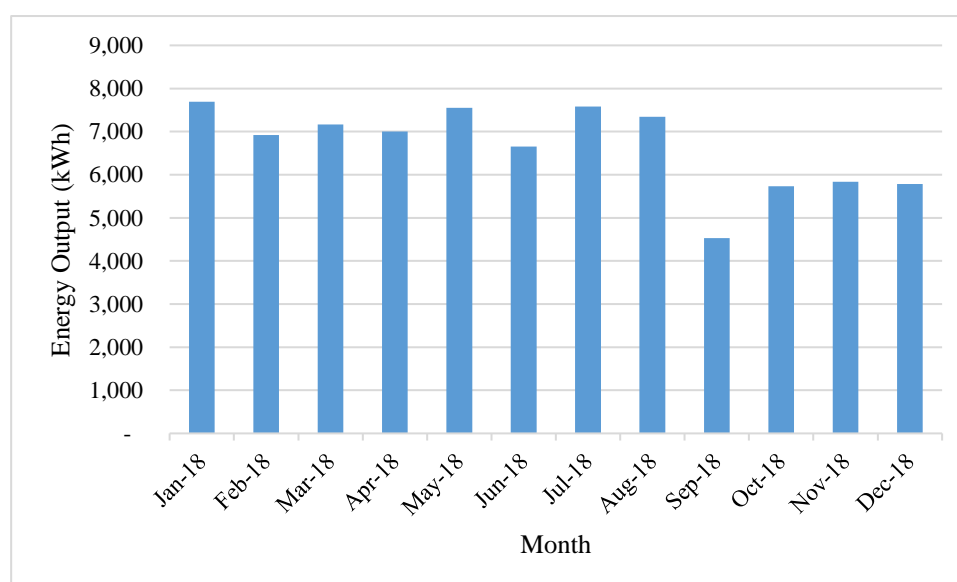


**Figure 2.18 Monthly energy output in 2018.**

## **2.4 Discussions**

The results indicated that OP plot which was free from shading has the highest grain yield at 839 g/m<sup>2</sup>. In the AV plot, the grain yield was only 649 g/m<sup>2</sup> at harvest, it was decreased by 22.6%. Previous study also shown shading at different rice growing stages had effect on grain yield. Solar radiation at reproductive stage has greatest effect on grain yield, followed by ripening stage, and vegetative stage (Yoshida, 1981). Delayed harvests on 10 and 17 October also decrease the grain yield by 20.33% and 22.8% respectively. The objective to has delayed harvest (four and eleven days after normal harvest date) was hoped to increase the grain yield, but the results shown were not promising. As compared to the grain yield at four day after normal harvest (10 October) in AV plot, the grain yield increased slightly by only 2.9%. The grain yield at eleven day after normal harvest (17 October) decreased slightly by 0.19%. Total biomass also has the similar trend as grain yield. The highest total biomass was on OP plot. Delayed harvest in AV plots did not increase total biomass.

By comparison with the study by Homma et al. (2016) that indicated a 20% shading of solar panel will reduce the yield of rice by approximately 20%, same finding was also obtained from the farm experiment in this research. Horizontal ground projection value indicated 27.18% shading by solar panels on the rice crop in this experimental site in Chikusei city. This shading had reduced the rice yield by 22.6% if not delaying the harvest date.

## **2.5 Conclusion**

The result from the experiment indicated partial shading in AV had resulted reduction of grain yield by 22.6%. Even with delayed harvest in AV plot, the reduction of grain yield was between 20.3% to 22.8%. Reduction of grain yield in AV plots was partly ascribed to the lower head number as compared to OP plot.

## **Chapter 3: Calibration and validation of models for light distribution, rice growth and power generation in AV system**

### **3.1 Introduction**

After conducting field experiment, field data were used for calibration and validation of the models. Modelling is the use of equations or sets of equations to represent the behaviour of a system (Patricia et al., 2012). In this study, three models were used for simulation, i.e., solar radiation model, crop growth model, and solar energy model. The model used for solar radiation simulation was Autodesk Revit with the integration of visual programming tool in Dynamo. Revit and Dynamo were used to simulate daily solar radiation under AV and then compare with observed data.

The crop growth model used in this study was APSIM-Oryza. It was used to simulate rice growth in the experimental field and in partial shading condition such as in AV. The third model for solar energy simulation was PVSyst. PVSyst was used to simulate monthly solar energy generation with different tilt angles settings.

### **3.2 Solar radiation model**

The estimation of light distribution is very important under AV system. Partial shading caused by solar photovoltaic panels will have different incoming of solar radiation. Therefore, solar radiation model was used to estimate the light distribution on crop canopy under AV system. Autodesk Revit and Dynamo software were chosen as it can simulate the incoming solar radiation. Autodesk Revit is a leading building information modelling software (Kensek, 2015). The software can be used to design a building, structure, its components in 3D. Then, annotate the model with 2D drafting elements, and access the building information from the model's database.

In AV, radiation reduction plays a pivotal role as it affects the microclimate under solar panel and excessive shading may reduce the growth rate of the crop (Marrou et al, 2013). In this study, a 3D model of AV was drawn in Autodesk Revit with different pre-defined angles. Autodesk Revit was not able to input weather data since they were using the default weather database from an external database in World Meteorological Organization (WMO) or from virtual weather station. Dynamo is a visual programming tool was used to shape the input weather data collected from weather station and simulate daily solar radiation.

### 3.2.1 Materials and methods: Model calibration and validation for Autodesk Revit and Dynamo

A 3D structural model of AV was drawn in Autodesk Revit version 2019 (<https://www.autodesk.com/products/revit/overview>). The 3D model mainly content three objects i.e. solar photovoltaic panel, vertical and horizontal structure poles. The object dimensions were summarized in (Table 3.1). The solar photovoltaic panel was drawn using roof component while structure poles using wall component. The tilt angles were changed as defined in Chapter 2. The width of solar photovoltaic panel was modified each time when changing the tilt angle due to trigonometry calculation of roof component in Revit and ensure the solar photovoltaic panel area is always  $0.763 \text{ m}^2$ . Figure 3.1 showed 3D view of AV.

**Table 3.1 Summary of object dimensions used in Revit.**

	<b>Length</b> (mm)	<b>Width</b> (mm)	<b>Depth</b> (mm)	<b>Thickness</b> (mm)	<b>Height</b> (mm)
<b>Solar Photovoltaic Panel</b>	1482	515		35	
<b>Vertical Structure Pole</b>	37.5	37.5			3500
<b>Horizontal Structure Pole</b>	35,000	37.5	37.5		

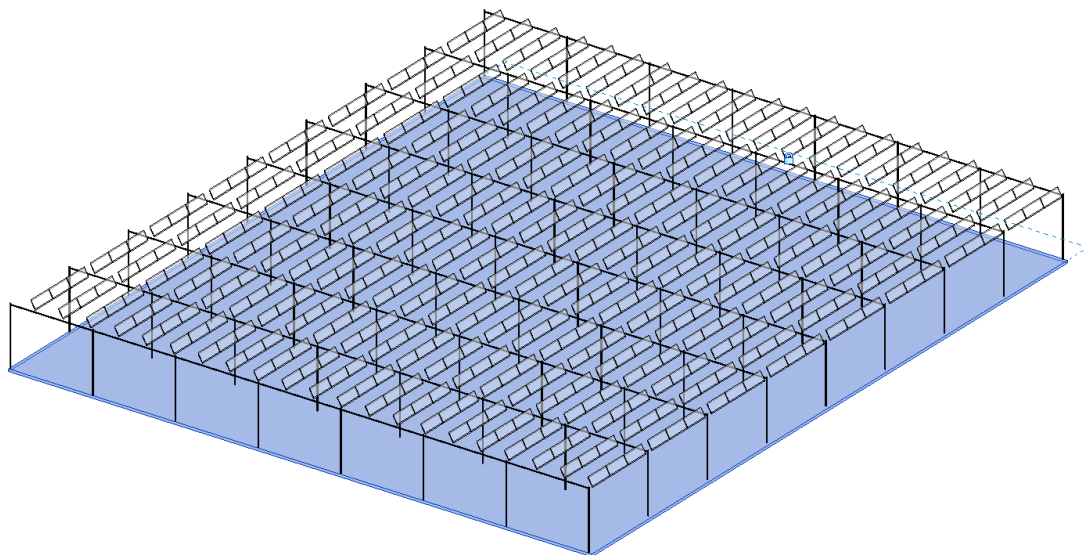


**Figure 3.1 3D views of AV**

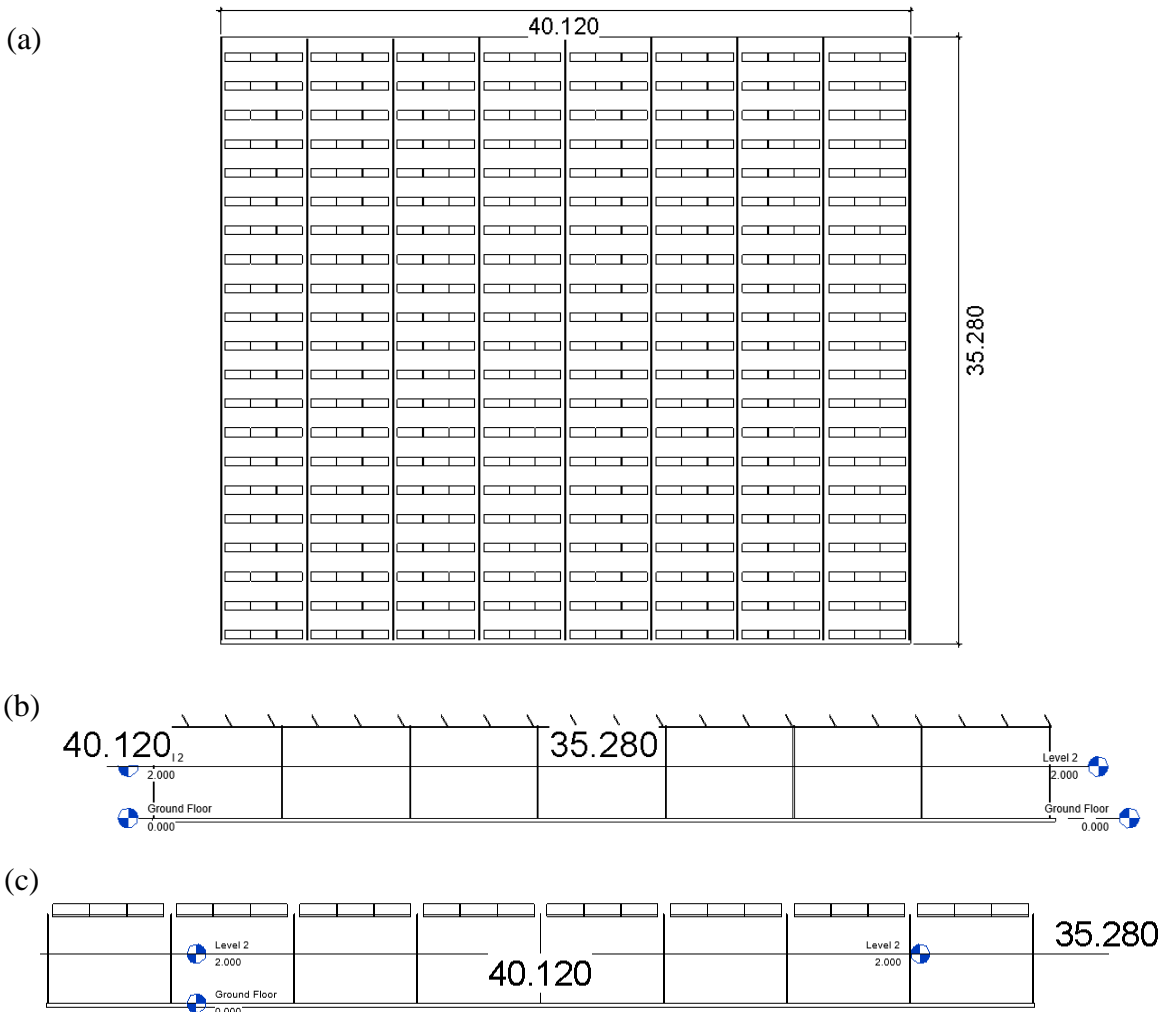


**Figure 3.2 (a) top view, (b) side view at tilt angle 60°, (c) front view at tilt angle 60°.**

Dynamo version 1.3.3.4111 was used for the simulation (<https://dynamobim.org/>). In Dynamo model, five main components were used to run the daily solar radiation simulation. These components included solar analysis, weather file, select surfaces, time study and export data. Among these components, the most important component is “Solar Analysis” node (Figure 3.3). The solar analysis node is based on the Perez All-Weather Sky Model. It is a mathematical model used to describe the relative luminance distribution of the sky dome. The grid size used in this simulation was 0.5 m. Weather data was collected from Meteonorm version 7.3.2 (<https://meteonorm.com/>) and it was based on Baseline Surface Radiation Network (BSRN) Tateno weather station. Tateno weather station is 41.5 km from the experiment field which is in the same location as JMA Tsukuba weather station. This weather data was selected because it contents contained daily direct horizontal radiation, direct normal

radiation, and diffuse radiation in “.wea” format which is required by Dynamo to run simulation. Figure 3.3 showed visual programming nodes in Dynamo.

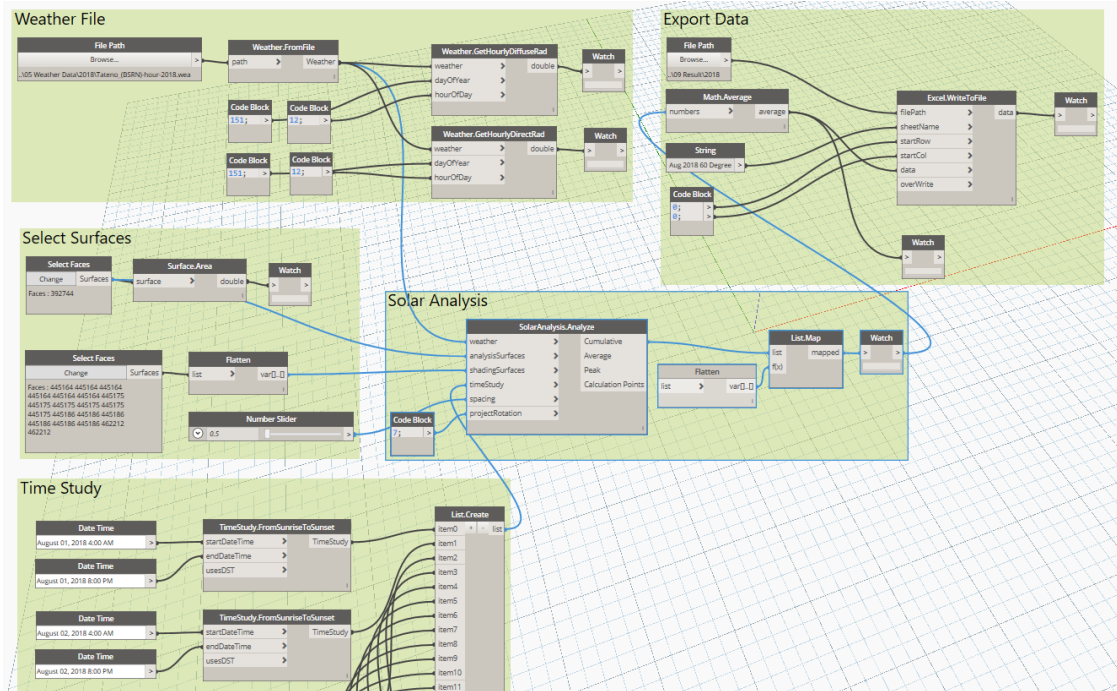


**Figure 3.3 Visual programming nodes in Dynamo.**

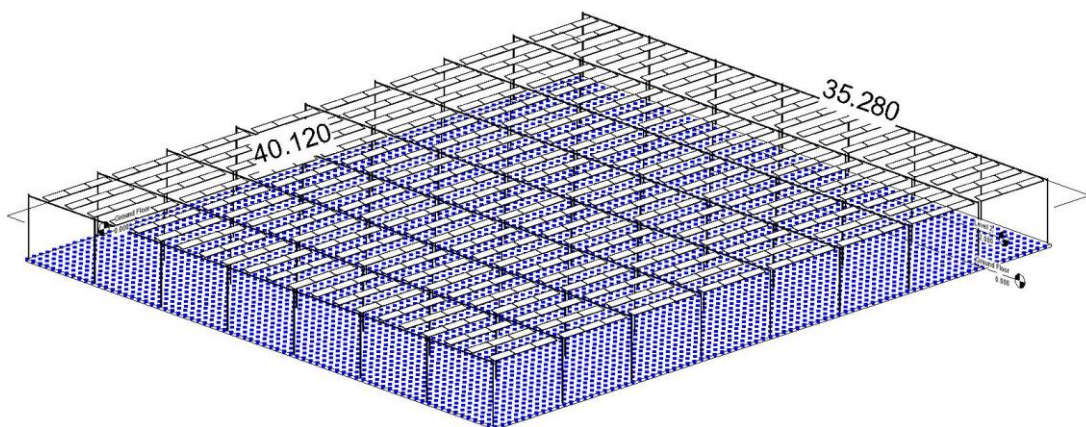


**Figure 3.4 3D model with simulation grid size (0.5 m) and tilt angle (10°) in Revit.**

### 3.2.2 Results and discussion

Figure 3.5 showed the comparison of simulated and observed solar radiation in AV from 2 August to 5 October. The correlation of determinant ( $R^2$ ) at 0.7873 showed a certain variability of data around mean but indicating good fit of the model.

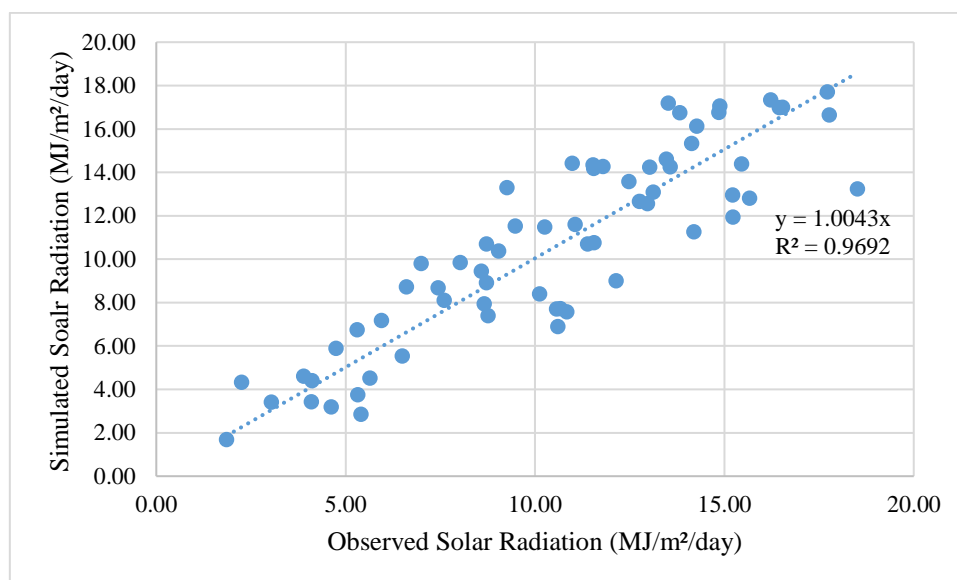


**Figure 3.5 Comparison of simulated and observed solar radiation in AV from 2 August to 5 October. Dotted line denotes 1:1 line.**

## 3.3 Crop growth model

APSIM-Oryza is a crop growth model that had been widely used to simulate rice growth in rainfed and irrigated conditions. The worldwide usage and increasing citations for Oryza model has established it as a robust and reliable model for predicting the growth and yield of rice (Li et al., 2017). APSIM-Oryza model had been adopted to simulate yield across major rice producing areas in the Asia and world (Gaydon et al., 2017). In this research, crop model APSIM-Oryza was used to estimate rice yield under irrigated environment under AV.

### 3.3.1 Model parameterization, calibration and validation for APSIM-Oryza

A model is a simplified representation of a system, while a system is a limited part of reality that contains interrelated elements (Penning de Vries & van Laar, 1982). Calibration of the model is a prerequisite for any study that uses crop model. Calibration is a process by which

parameters are estimated so that the output of the overall model matches expected results. As such, models are tested using different values for a specific parameter and final values are chosen based on the closest match to the observations of the major outputs (Soltani & Sinclair, 2012). Parameter estimations are required when crop parameter used in the study is not readily available through literature for that specific cultivar. Therefore, cultivar specific parameters responsible for phenology, dry matter production and grain yield are adjusted to match the observed values. Some general parameters are also adjusted that indirectly affect the cultivar specific parameters if required. Data collected from field experiment in the same soil and climatic condition will be used for calibration.

Cultivar parameter or genotypic coefficients are used to define varietal difference in the APSIM-Oryza model. Genotypic coefficients are variety specific; it should be derived with a trial-and-error method by matching the simulated and observed flowering and maturity dates (Wang et al., 2013). Since the genotypic coefficient values of the variety used (Asahi-no-yume) were not available in the literature, a trial-and-error method was used to derive the required parameters.

### 3.3.2 Materials and methods

APSIM model version 7.9 was used for this study. Files required for APSIM-Oryza simulation were downloaded from the APSIM webpage (downloaded on 1 May 2019). Workshop materials in the training manual (South Asia) were selected as these materials were used for rice simulation. “Rice single season.apsim” file was selected and modification was done on the “Transplanted-paddy\_rice1” component. The “Transplanted-paddy\_rice1” component was selected due to the built-in puddling effect. Since the experimental field was using transplanting and irrigation, the selected component is suitable for this study. The puddling effect was verified by checking saturated hydraulic conductivity (Ks) in the water node of silt under the paddock component. The default values at depths of 15-30 cm (second layer) was set to 1 mm day<sup>-1</sup> to represent the puddling effect in soil. Saturated hydraulic conductivity indicates the rate when water flowing down to the next soil layer under saturated soil water conditions. Puddling is effective to reduce the saturated hydraulic conductivity of the soil layer and thus decrease the percolation rate significantly (Tuong et al., 1994). APSIM-Oryza model was first initialized using weather and soil data and then crop management.

### 3.3.2.1 Weather parameters

Daily weather data (daily precipitation, maximum and minimum temperatures) collected from JMA Shimodate Weather Station were used. Since solar radiation data was not available in Shimodate Weather Station, solar radiation data from Tsukuba Weather Station was used for this simulation.

### 3.3.2.2 Soil parameters

Soil data for the experimental field were obtained from SoilGrids, International Soil Reference and Information Centre (ISRIC). The soil data was based on the geographical coordinates from (<https://soilgrids.org>). Initial soil water content was set to 100% and filled from the top. Air Dry (mm/mm) values were set to half of LL15 (mm/mm) values. Soil water data were estimated using the soil texture formula as described by (Saxton & Rawls, 2006) and showed in (Table 3.2). Initial nitrogen for soil layers at 0 to 90 cm were modified (Table 3.3). As Japanese soil parameters are not included in APSIM soil database, the chosen soil type was modified to represent volcanic ash soil type (Nuwan, 2018). FBiom (proportion of non-inert carbon in microbial biomass pool) and FInert (Proportion of initial organic carbon assumed to be inert) soil parameters were adjusted by comparing with observed dry matter production values at the flowering and maturity stages (Table 3.4).

**Table 3.2 Soil Water**

<b>Depth of soils (cm)</b>	<b>Bulk Density (g/cm<sup>3</sup>)</b>	<b>Air Dry (mm/mm)</b>	<b>LL15 (mm/mm)</b>	<b>DUL (mm/mm)</b>	<b>SAT (mm/mm)</b>	<b>Ks (mm/day)</b>	<b>pH (1:5 water)</b>
0-15	1.20	0.063	0.127	0.241	0.393	220.376	5.90
15-30	1.35	0.065	0.130	0.247	0.394	1.000	6.05
30-60	1.40	0.068	0.136	0.251	0.395	188.705	6.15
60-90	1.40	0.071	0.142	0.255	0.396	175.373	6.25

**Table 3.3 Initial Nitrogen**

Depth of soils (cm)	NO <sub>3</sub> <sup>-</sup> (kg/ha)	NH <sub>4</sub> <sup>+</sup> (kg/ha)
0-20	12.0	8.0
20-90	8.0	2.0

**Table 3.4 Soil Organic Matter**

Depth of soils (cm)	Organic C Content (Walkley & Black %)	FBiom (0-1)	FInert (0-1)
0-15	2.40	0.030	0.500
15-30	1.90	0.030	0.500
30-60	1.25	0.020	0.500
60-90	0.80	0.010	1.000

### 3.3.2.3 Crop management in model simulation

Crop management was defined according to farmer's practice. Sowing window was set at 16 April as described in Chapter 2. Number of plants per hill was set to 3 and number of hills per area was 18 m<sup>-2</sup>. Number of plants per seed bed was set at 1,000. Since the rice field was with irrigation, pond depth setting is required. Ponding and irrigation dates were set from 11 May (transplanting) to 30 September (one week before harvest) respectively. The water in the field was drained one week before harvest to dry the soil and to ease movement of combine harvester in the field. Double ponding depth at different date was not allow in APSIM-Oryza, so the maximum pond depth was set to 150 mm and minimum pond depth was 100 mm throughout the irrigation period. Maximum number of irrigations was set at 30 and this value was enough to maintain the required pond depth. Basal fertilizer (NH<sub>4</sub>-N) was applied on transplanting date at the amount of 48 kg/ha. Top-dressing fertilizer (NH<sub>4</sub>-N) at 12 kg/ha was applied on 31 July when the temperature was almost at the highest during the growing season to break down granular fertilizer and easily absorbed by plant.

#### 3.3.2.4 Deriving cultivar parameters

In APSIM-Oryza file, twelve default rice cultivars are available for selection. Among these cultivars, only one cultivar is belonging to Japonica rice cultivar. The Japonica rice cultivar is Wuxiangjing with large panicles and high yield potential (Yang et al., 2008). This cultivar was selected as base cultivar and the parameters were further calibrated for rice cultivar Asahi-no-yume.

#### 3.3.2.5 Calibration process and target phenology parameters

The following processes were applied to parameterize cultivar parameters through step-by-step and trial-and-error method to minimise RMSE of the differences between the observed and simulated variables. About 10% of the crop parameters are expected to be adjusted depending on the targeted cultivar (Bouman & van Laar, 2006) in ORYZA2000.

#### 3.3.2.6 Phenological development

Development stage (DVS) of a plant define the physiological age and characterized by formation of the various organs and their appearance. The most important phenological change is from vegetative to the reproductive stage, as it determines the change in dry matter allocation over organs. Since many physiological and morphological processes change with the phenological stage of the plant, quantification of phenological development accurately is essential in any simulation model for plant growth (Bouman et al., 2001).

The life cycle of the rice crop is divided into four main phenological phases. First is the basic vegetative phase (BVP), from emergence (DVS = 0) to the start of the photo-period-sensitive phase (DVS = 0.4). The development rate constant in this phase is expressed as DVRJ. Second phase is photoperiod-sensitive phase (PSP), from the end of basic vegetative phase to panicle initiation (DVS = 0.65). The development rate constant in this phase is expressed as DVRI. Third phase is the panicle formation phase (PFP), from panicle initiation to (50%) flowering (DVS = 1). The development rate constant in this phase is expressed as DVRP. The last phase is grain-filling phase (GFP), from (50%) flowering to physiological maturity (DVS = 2). The development rate constant in this phase is expressed as DVRR. The development stage is the integral of the development rate (DVR) over time and expressed in degree-days (°Cd). The development rate of the crop is calculated based on the development rate constants

for different phenological stages, the daily increment in heat units (HU; °Cd d<sup>-1</sup>), and the photoperiod (Bouman et al., 2001).

Among these four phenological phases, calibration was done on the development stages at DVRJ and DVRR only to match the flowering and maturity (Table 3.5). Maturity date was assumed to be same as the date of harvest.

**Table 3.5 Phenological Parameter Values for Asahi-no-yume**

<b>Phenology Parameters</b>	<b>Default Value</b>	<b>Adjusted Values</b>
DVRJ- Development rate in juvenile phase (°Cd <sup>-1</sup> )	0.000773	0.00085
DVRI- Development rate in photoperiod-sensitive phase (°Cd <sup>-1</sup> )	0.000749	Remained
DVRP- Development rate in panicle development phase (°Cd <sup>-1</sup> )	0.000785	Remained
DVRP- Development rate in reproductive phase (°Cd <sup>-1</sup> )	0.001281	0.00143

### 3.3.2.7 Dry matter partitioning

In APSIM-Oryza, dry matter produced by the crop is partitioned between shoots and roots according to partitioning coefficients defined as a function of the phenological development stage. FSH is fraction of dry matter partitioned to shoot and FRT is fraction dry matter partitioned to roots. Dry matter allocation to the shoot is further partitioned to the various groups of plant organs. FLV is the fraction dry matter partitioned to the leaves, FST to the stems, and FSO to the storage organs, all as fraction of shoot dry matter growth. All partitioning coefficients are interpolated from partitioning tables read in the initialization section (Bouman et al., 2001). Among the partitioning factors, only FSO was adjusted to match flowering stage (DVS = 1) of biomass and grain yield (Table 3.6).

**Table 3.6 Fraction Dry Matter Partitioned to Storage Organ (FSO) for Rice Cultivar Asahi-no-yume**

Development Stage (DVS)	Emergence			Flowering		
FSOT- FSO as function of Development Stage	0.00	0.50	0.75	1.00	1.20	2.50
FSO- Fraction of shoot dry matter allocated to storage organs (Default Values)	0.00	0.00	0.00	0.60	1.00	1.00
FSO (Adjusted Value)	0.00	0.00	0.00	0.80	1.00	1.00

### 3.3.3 Methods of model evaluation

After obtaining parameters through calibration process as described above, the phenology parameter was taken as target cultivar (Asahi-no-yume). Observed and simulated grain yield, and dry matter production were compared graphically. Date of flowering and maturity were compared in a table. The model performances were quantified using three statistical indices which widely used in previous research (Wang et al., 2013) and (Gaydon et al., 2017), iel, root mean square error (RMSE), relative root mean square error (RRMSE), and modelling efficiency (EF). RMSE measures the absolute magnitude of the error. RMSE has the same unit of the observed and simulated values. RMSE closer to 0 indicates the best model performance, a lower RMSE value denotes better performance. RRMSE is used to compare simulation quality of data with highly different averages for example grain yield in  $g/m^2$  and the unit is independent. RRMSE is calculated by dividing the RMSE by the mean of the observed values and expressed as percentage (Nuwan, 2018). Lower RRMSE value indicates lesser residual variance. Residual variance measures how accurately the model's predictions match with observed value. Model accuracy is considered very good if  $RRMSE < 10\%$ , good if  $10\% < RRMSE < 20\%$ , fair if  $20\% < RRMSE < 30\%$ , and poor if  $RRMSE > 30\%$ , (Heinemann et. al, 2013) .

The modelling efficiency (EF) is also known as Nash-Sutcliffe modelling efficiency comparing the deviations between observed and simulated values to the variance of the observed values (Moriassi et al., 2007).  $EF = 1$  indicates perfect match of the simulated and observed values.  $EF = 0$  indicates the model predictions are as accurate as the mean of the

observed data, whereas an efficiency less than zero ( $-\infty < EF < 0$ ) indicates the observed mean is a better predictor than the model. EF values between 0 and 1 are generally regarded as acceptable levels of model performance. Model performance can be evaluated as satisfactory if  $EF > 0.5$ , good if  $EF > 0.65$ , and very good if  $EF > 0.75$  (Moriassi et al., 2007). Figure 3.6 shows the equations for calculating RMSE and EF.

RMSE = Root Mean Square Error

$$RMSE = \sqrt{\frac{\sum_{i=1,n} (S_i - O_i)^2}{n}}$$

Model Efficiency = EF

$$EF = 1 - \frac{\sum_{i=1,n} (O_i - S_i)^2}{\sum_{i=1,n} (O_i - \bar{O})^2}$$

where  $S_i$  = Simulated value,  $O_i$  observed value,  $\bar{O}$  = mean of observed value,  $n$  = number of observations.

(Source of equations: (Gaydon et al., 2017))

**Figure 3.6 Equations to calculate RMSE and EF.**

### 3.3.4 Results and discussion

#### 3.3.4.1 Total biomass and grain yield of rice

Table 3.7 showed the model performance of APSIM-Oryza. The simulated total biomass was slightly underestimate for the first three samplings during the rice growing stages but correlation of determinant ( $R^2$ ) is relatively high at 0.9832 (Figure 3.7). Overall model efficiency was very good at 0.95 (very good if  $EF > 0.75$ ). Simulated rice yields slightly underestimated (Table 3.8).

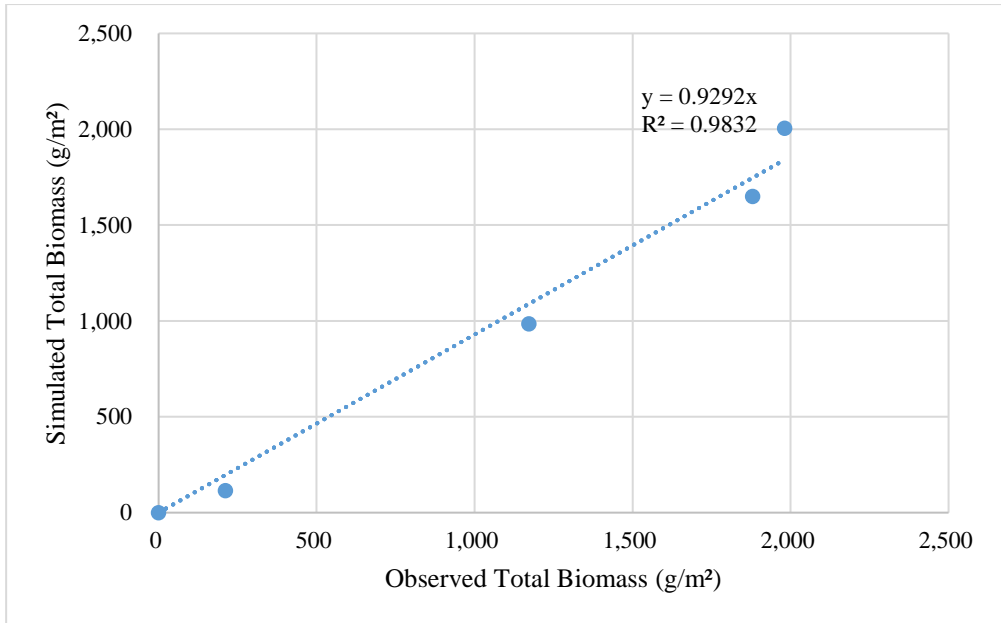


**Figure 3.7 Observed and simulated total biomass. Dotted line denotes 1:1 line.**

**Table 3.7 Summary of APSIM-Oryza model performance.**

	<b>RMSE</b>	<b>RRMSE</b>	<b>EF</b>	<b>Slope</b>	<b>R<sup>2</sup></b>
<b>Total Biomass (g/m<sup>2</sup>)</b>	156.75	11.95	0.951	0.9292	0.9832

**Table 3.8 Comparison of observed and simulated rice yield and total biomass.**

	<b>Observed</b>	<b>Simulated</b>
<b>Grain Yield (g/m<sup>2</sup>)</b>	839	809
<b>Total Biomass (g/m<sup>2</sup>)</b>	1,982	2,005

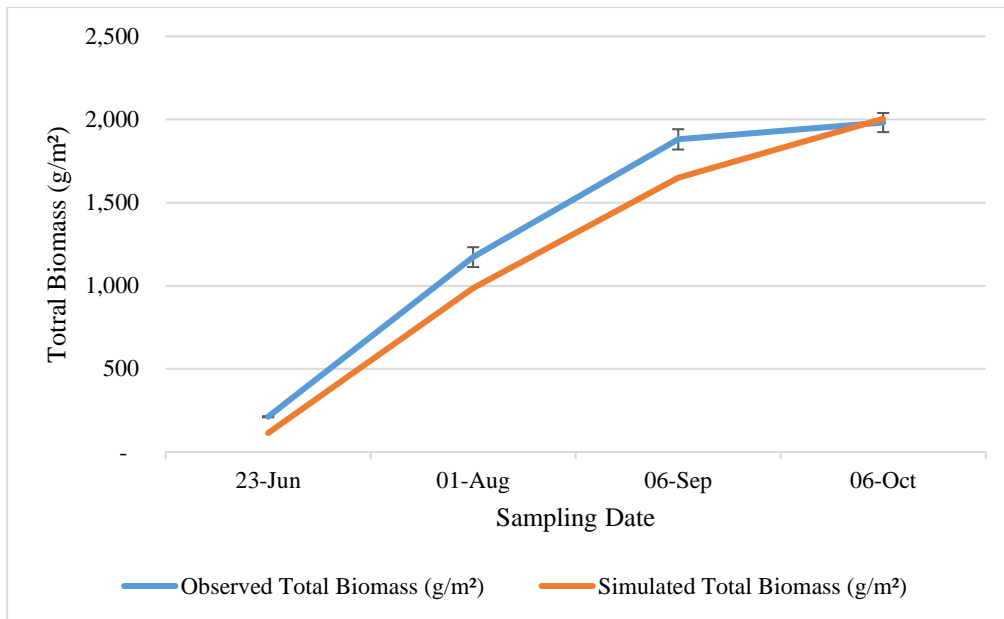


**Figure 3.8 Comparison of observed and simulated total biomass at different samplings date. Vertical bars denote the standard error.**

### 3.4 Solar energy model

In this research, one of the well-known and widely used software tool PVSyst is opted for evaluating the energy output of the solar panels in AV. PVSyst is a software developed by the University of Geneva (PVSyst). It integrates pre-feasibility, sizing and simulation support for PV systems. With the inputs of the weather data station and specifications of the solar panels and electrical components, PVSyst could automatically calculates the energy yield of the solar system. In the solar industry, various PVSyst simulation are carried out to analyse the energy output of solar panels either on the ground, mountain, rooftop or floating water application.

Kumar et al., (2017) presented the simulation of a 100kWp grid-connected solar photovoltaic system using PVSyst and performance. Meteonorm weather data sets of solar radiation and ambient temperature have been utilized to generate the energy output of the PV system. In addition, another PVSyst study on a 10 MWp grid connected solar power plant had showed a positive correlation with the monitoring result obtained from installed solar PV plant at the site (Kumar et al., 2017) . Dinesh and Pearce (2016) also utilized PVSyst coupled with a crop model (STICS) to ascertain the potential of AV in economic value. From the literature review, it is clear that PVSyst is widely used as a tool to investigate the energy yield from solar PV.

### 3.4.1 Materials and methods: model calibration and validation for PVSyst

Solar energy model was simulated according to the solar photovoltaic system configuration in Chapter 2. The tilt angle was following the pre-defined angle in Table 3.9. Soiling caused by dust and dirt was set at 3% according to the standard setting in PVSyst. Simulated and observed energy outputs were compared by calculating the correlation of determinant ( $R^2$ ).

**Table 3.9 Solar panels tilt angle**

Month	Jan	Feb	Mar	Apr	May	June	July	Aug	Sept	Oct	Nov	Dec
<b>Tilt Angle (°)</b>	60	51	36	20	10	10	10	14	25	42	55	60

### 3.4.2 Results and discussion

Total simulated energy output showed higher value than observed output by 4.87% (Table 3.10 Simulated and observed energy output in 2018. Table 3.10). However, correlation of determinant ( $R^2$ ) is relatively high at 0.9873 which means PVSyst model can simulate solar energy in AV (Figure 3.9).

**Table 3.10 Simulated and observed energy output in 2018.**

Tilt Angle (°)	Month	Observed Energy Output (kWh)	Simulated Energy Output (kWh)	Difference (%)
60	Jan-18	7,692	8,561	11.30
51	Feb-18	6,920	7,317	5.74
36	Mar-18	7,169	7,582	5.76
20	Apr-18	7,003	7,636	9.04
10	May-18	7,553	8,030	6.31
10	Jun-18	6,656	6,533	1.84
10	Jul-18	7,584	7,978	5.20
14	Aug-18	7,345	7,533	2.57
25	Sep-18	4,526	4,669	3.15
42	Oct-18	5,735	5,652	1.45
55	Nov-18	5,838	5,983	2.48
60	Dec-18	5,787	6,221	7.49
	<b>Total</b>	<b>79,807</b>	<b>83,695</b>	<b>4.87</b>

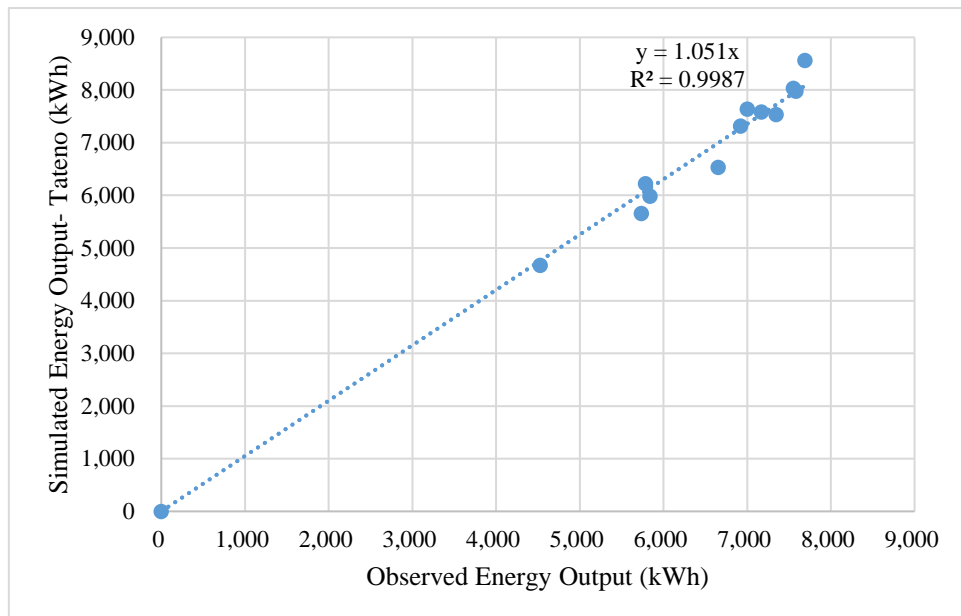


**Figure 3.9 Comparison of observed and simulated energy output (kWh). Dotted line denotes 1:1 line.**

### **3.5 Conclusion**

From the simulation result of solar radiation models, the  $R^2$  is at 0.7873 which indicates Revit and Dynamo models can simulate solar radiation in AV quite accurately. The performance of crop growth model (APSIM-Oryza) showed a high model efficiency at 0.95 and total biomass's  $R^2$  at 0.9832. Solar energy model (PVSyst) showed  $R^2$  at 0.9873 which also indicate a reliable model to estimate energy output. In short, these three models give a reliable estimation.

## Chapter 4: Scenarios analysis for economically optimum rice and energy production in agrivoltaic system

### 4.1 Introduction

Farmers and solar farm developers or energy investors are looking for optimization of rice and energy production under AV. However, current research lack of proof of economic benefit from AV. In this section, scenario analysis is performed to understand the economically optimum rice and energy production in AV. With this information, farmers and investors therefore can wisely evaluate the monetary benefit of AV.

AV in Chikusei city rice field has been installed with varies pre-defined tilt angles at different months as shown in (Table 4.1). In the scenario analysis, different tilt angles are selected to simulate the rice and energy output using the validated values from solar radiation (Revit & Dynamo), crop growth (APSIM-Oryza) and solar energy (PVSyst) models.

**Table 4.1 Solar panels tilt angle**

Month	Jan	Feb	Mar	Apr	May	June	July	Aug	Sept	Oct	Nov	Dec
<b>Tilt</b>												
<b>Angle</b>	60	51	36	20	10	10	10	14	25	42	55	60
(°)												

From literature review in Chapter 1, it was reported that the critical period for sunlight in rice growth started from panicle initiation to medium drough stages. Within this period, the first heading stage required the highest cumulative sunlight. In the experimental field, heading date was identified on 17 August 2018. Therefore, scenario analysis focus on the month of August which required highest cumulative sunlight in rice growth stage. It is aimed to find the optimum distribution of solar radiation between solar panels and rice crop by adjusting the tilt angle of the solar panel in the month of August. The result from scenario analysis can provide decision support making to farmer and energy investors when integrating solar photovoltaic in the rice field.

## 4.2 Scenario analysis of solar radiation at different tilt angles

### 4.2.1 Materials and methods

Revit and Dynamo models were used to simulate solar radiation under AV at tilt angle 25°, 42° and 60° in the month of August to compare with the default tilt angle of 14°. Weather data from BSRN Tateno weather station year 2018 was used for the simulation. The simulated cumulative daily solar radiation in August gained from Revit and Dynamo models was then utilized as the input weather file in APSIM-Oryza simulation.

### 4.2.2 Results and discussion

Solar radiation simulation results from Revit and Dynamo models clearly indicated that lowest solar panels tilt angle (14°) in August has the lowest solar radiation at rice canopy which is at total 418 MJ/m<sup>2</sup> per month (Table 4.2). When performing the scenario analysis, tilt angle was adjusted from 14° to 25°, 42°, and 60°. The result showed that the solar radiation at crop canopy at 60° had the highest value at total 445 MJ/m<sup>2</sup> per month. The result is justifiable since August is the summer season in Japan and sun's path is higher in the sky. Apparently, a low tilt angle (14°) will block sunlight reaching crop canopy under solar panels and made the crop receive lesser sunlight. In contrast, a higher tilt angle at 60° will allow more sunlight reaching the canopy of rice crop from top.

**Table 4.2 Comparison of simulated solar radiation in August**

<b>Tilt Angle (°)</b>	<b>14 (default)</b>	<b>25</b>	<b>42</b>	<b>60</b>
<b>Simulated Solar Radiation (MJ/m<sup>2</sup>)</b>	418	420	429	445

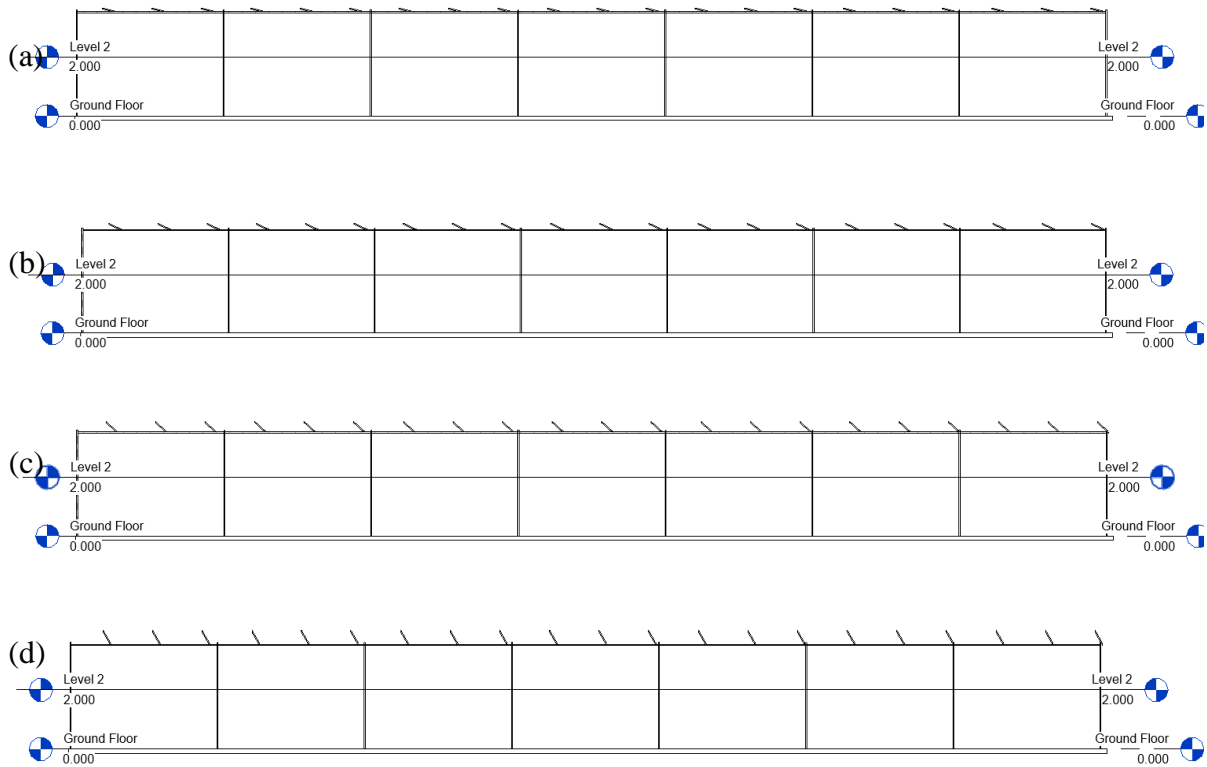


**Figure 4.1 Solar photovoltaic tilt angle at (a) 14°, (b) 25°, (c) 42°, (d) 60°.**

### 4.3 Scenario analysis of rice yield at different tilt angles

#### 4.3.1 Materials and methods

The simulated solar radiation data in August from Revit and Dynamo was used as the input weather file in APSIM-Oryza model while maintaining other months' solar radiation. Soil data, crop management practices, and rice cultivar were all maintained the same. Simulation was carried out at 25°, 42° and 60° in the month of August and compared with the default tilt angle to determine the effect of partial shading on rice yield and total biomass.

#### 4.3.2 Results and discussion

Figure 4.2 showed the simulated grain yield and total biomass at 25°, 42° and 60° on August as compared to the default tilt angle 14°. The highest simulated grain yield (7.411 t/ha) was gained from the tilt angle 60°. This indicated an increment of grain yield by 3.84% from the default tilt angle (Figure 4.3). Similarly, highest simulated total biomass (17.53 t/ha) was

also observed at the tilt angle 60°. The highest grain yield and total biomass at tilt angle 60° could be explained by the highest solar radiation received by crop.

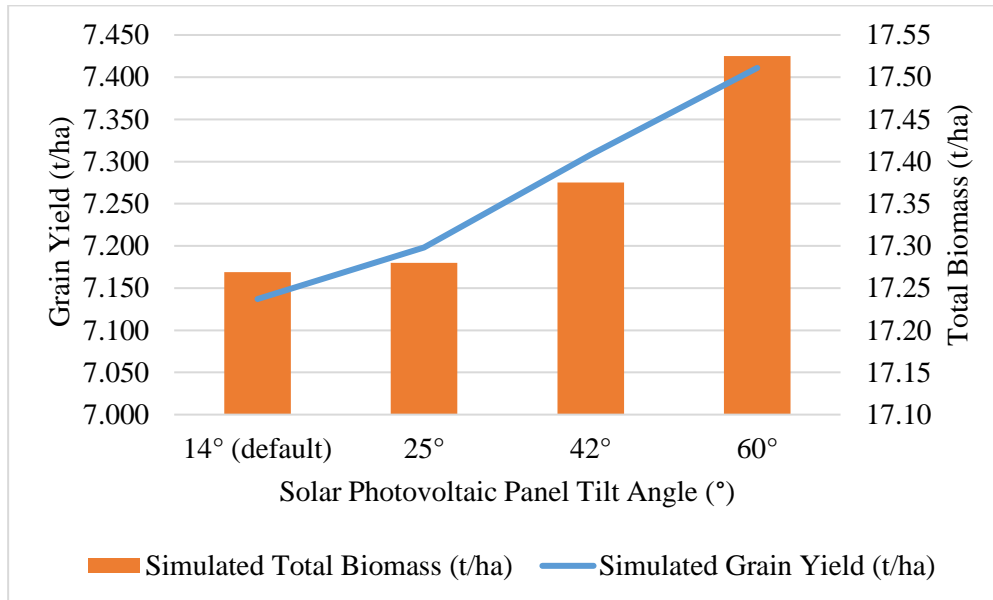


**Figure 4.2 Comparison of simulated grain yield and total biomass at 14°, 25°, 42° and 60° in August.**

Tilt Angle (°) on August	Simulated Grain Yield (t/ha)	Difference of Yield (%)	Simulated Total Biomass (t/ha)	Difference of Total Biomass (%)
14° (default)	7.137		17.27	
25°	7.198	0.85	17.28	0.06
42°	7.308	2.40	17.38	0.61
60°	7.411	3.84	17.53	1.48

**Figure 4.3 Difference of simulated grain yield and total biomass at 14°, 25°, 42°, 60° in August.**

In order to compare monetary value of rice at different tilt angles, the simulated grain yield was converted to rice selling price. The selling price of brown rice from farmer to Japan Agricultural Cooperatives (JA) was set at 13,000 JPY/60kg in 2018. It was equivalent to 217 JPY/kg. This data was collected during the interview with farmer of Chikusei farm. In the rice field experiment, total area under AV was 1415 m<sup>2</sup>. The highest monetary value from rice selling was 227,633 JPY when solar photovoltaic panel is at tilt angle 60° (Table 4.3). This showed an increment at 3.85% when adjusted tilt angle from 14° to 60°. Data from the field experiment showed the decrease of 22.6% of rice yield when it is tilted at 14°. However, rice yield will increase by 3.85% if tilted to 60°. In total, rice yield decrease is only 18.75% if tilted at 60°. This result showed the rice yield decrease would be less than 20% and this will meet the requirements set by MAFF.

**Table 4.3 Simulated grain yield and rice selling amount**

<b>Tilt Angle (°) on August</b>	<b>Simulated Grain Yield (kg/m<sup>2</sup>)</b>	<b>AV Area (m<sup>2</sup>)</b>	<b>Simulated Grain Yield under AV Area (kg)</b>	<b>Rice Selling Amount (JPY)</b>	<b>Difference of Rice Selling Amount (%)</b>
14° (default)	0.7137	1,415	1,010	219,170	
25°	0.7198	1,415	1,019	221,123	0.89
42°	0.7308	1,415	1,034	224,378	2.38
60°	0.7411	1,415	1,049	227,633	3.86

Note: Brown rice selling price is 217 JPY/kg.

## 4.4 Scenario analysis of energy output at different tilt angles

### 4.4.1 Materials and methods

Solar energy model (PVSyst version 6.81) was used to run scenario analysis at different tilt angles. The similar solar photovoltaic system configuration was applied as described in Chapter 2 and 3. Soiling caused by dust and dirt was set at 3% according to the standard setting in PVSyst. Plane azimuth angle was set as -7°. Figure 4.5 showed PVSyst user interface for

project designation. Figure 4.5 showed field parameters input and Figure 4.6 showed global system configuration.

Three tilt angles were selected for scenario analysis and compared with the default angle. Tilt angle 25° was selected as first scenario analysis because of the optimum angle in September is 25°. If higher than this angle, solar energy generation will reduce. Second scenario analysis was based on tilt angle 42°. This angle (42°) was the next optimum angle in the following month (October). The scenario analysis is to test the maximum optimum angle range between month and select the highest energy output. The third scenario was based on 60° which is the highest angle in a year. It was selected to determine the maximum increase or decrease of the solar energy output.

After simulated the solar energy at 25°, 42°, and 60°, the simulated values were compared with the default tilt angle of 14°. Then, the energy output was converted into monetary value. The feed-in tariff (FIT) rate adopted for this AV is 32 JPY/kWh.

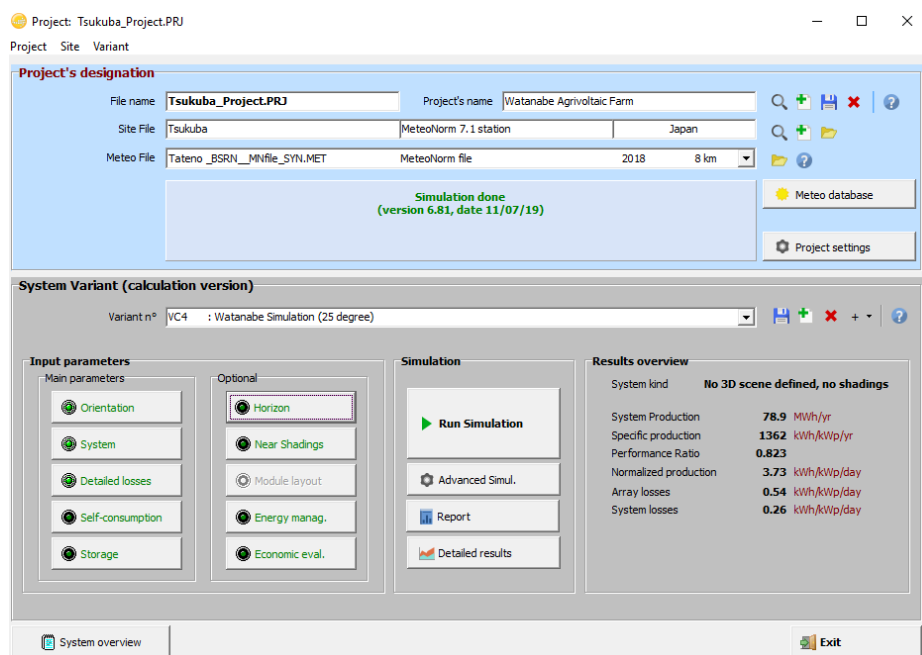


Figure 4.4 PVSyst user interface on project designation.

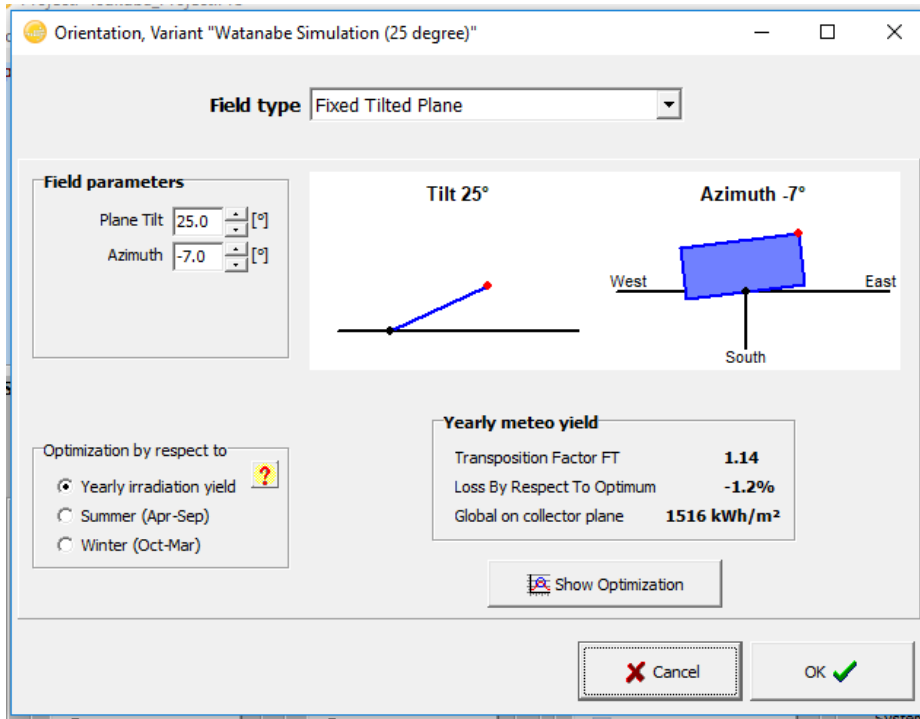


Figure 4.5 PVSyst user interface on field parameters.

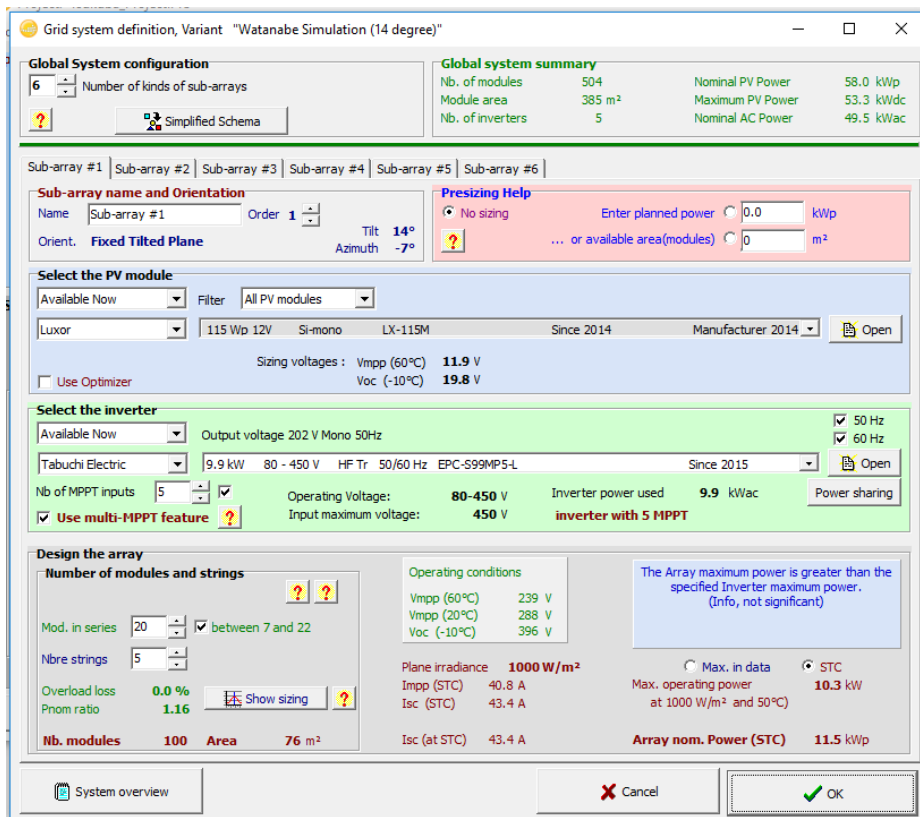


Figure 4.6 Global system configuration

#### 4.4.2 Results & discussion

The simulated result indicated that tilt angle 14° was the optimum angle for energy generation with the energy output of 7,532 kWh. When the tilt angle increased to 25°, simulated output reduces to 7,497kWh, 42° (7,071 kWh), and 60° (6,128 kWh). The highest energy selling amount was at tilt angle 14° and the amount was 241,024 JPY. The selling amount dropped by 18.6% when tilted to 60° in August (Table 4.4 and Figure 4.7).

This simulated result is consistent with current pre-defined tilt angle 14° set at Chikusei farm in August for optimum solar energy generation. The tilt angle 14° was used for the last three years since the installation in 2016. This proved that PVSyst is a reliable solar energy simulation model that enable to estimate solar energy output in AV.

**Table 4.4 Simulated energy output (kWh) at different angles in August.**

<b>Tilt Angle (°) on August</b>	<b>Simulated Energy Output (kWh)</b>	<b>Energy Selling Amount (JPY)</b>	<b>Difference in Energy Selling (%)</b>
14	7,532	241,024	
25	7,497	239,904	-0.5
42	7,071	226,272	-6.1
60	6,128	196,096	-18.6

Note: Energy selling price under feed-in tariff scheme is 32 JPY/kWh.

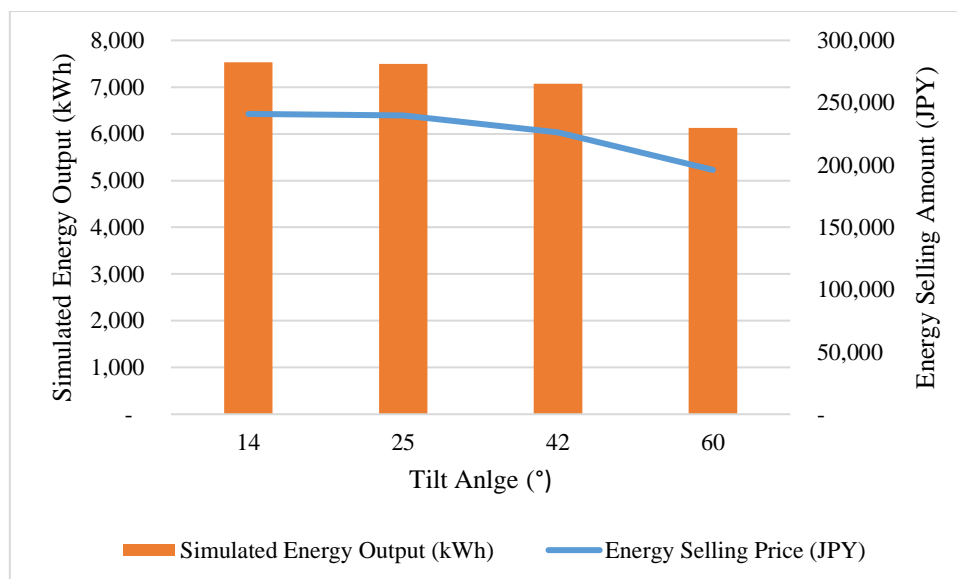


**Figure 4.7 Simulated energy output (kWh) at different angles in August.**

Note: Energy selling price under Feed-in Tariff scheme is 32 JPY/kWh.

#### 4.5 Economically optimum rice and energy production

Evaluation results on economic optimum of AV is described herein, where results from scenario analysis using tilt angle 14° (default), 25°, 42° and 60° are analysed. Energy selling from May to October (during rice growing season) was compared at different tilt angles. Rice selling amount at different tilt angles were also analysed. Comparing four scenarios, it emerged that solar panels tilted at 14° in the month of August reached the highest energy selling amount at of 1,080,128 JPY during rice growing season. In contrast, highest rice selling amount was at 60° at 221,123 JPY during the rice growing season

To analyse economically optimum of rice and energy production, both energy and rice selling amount were added together. It appeared that tilt angle 25° provides the maximum economical return at 1,300,133 JPY in the rice growing season from May to October (Table 4.5). It is about 0.06% increase in the monetary value if compared with the current tilt angle of 14° in AV field. Figure 4.8 showed total rice and energy selling amount from May to October 2018.

**Table 4.5 Rice and energy selling amount from May to October 2018.**

August Tilt Angle (°)	Energy Income (JPY)	Rice Income (JPY)	Total Income (JPY)	Difference (%)
14	1,080,128	219,170	1,299,298	
25	1,079,008	221,123	1,300,131	0.06
42	1,065,376	224,378	1,289,754	-0.73
60	1,035,200	227,633	1,262,833	-2.81

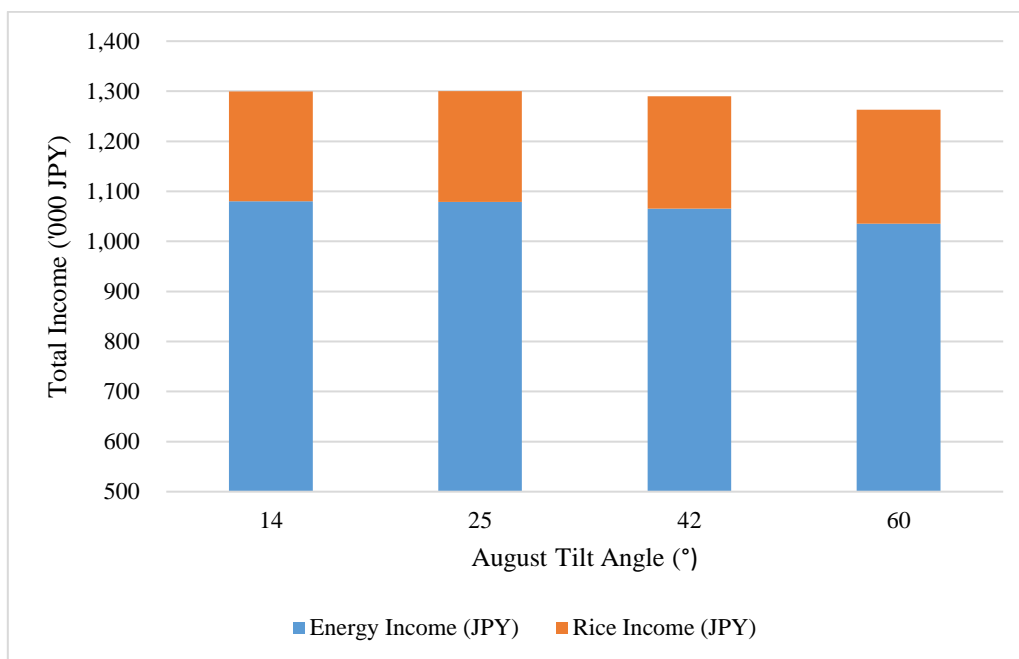


**Figure 4.8 Total rice and energy income from May to October 2018.**

## 4.6 Conclusion

The scenario analysis had concluded the best tilt angle to gain optimum rice and energy production is 25°. The result clearly provides an important information to the existing farmer who had operated the AV in Chikusei farm since 2016. With this novel finding of optimum tilt angle of 25°, farmer will gain slightly more monetary benefit (0.06%) from both rice and energy production.

The result also successfully validates the modelling approaches using Revit & Dynamo, APSIM-Oryza, and PVSyst could be a robust approach to obtain the economically optimum rice and energy production under AV. This help the farmers and energy investors to be able to better forecast their monetary income from AV by applying the modelling approaches.

## **Chapter 5: General discussion and conclusion**

### **5.1 Partial shading on rice yield in AV**

The result from field experiment showed rice yield reduction under partial shading condition in AV was 22.6% compared with OP with full sunlight. Delayed harvest was carried out on the fourth days and eleventh days after normal harvest. It was expected that delayed harvest could increase rice yield by the accumulation of more solar radiation. However, the result was negative. Even with the delayed harvest, rice yield reduction was in between 20.3% (four days after normal harvest) to 22.8% (eleven days after normal harvest). The reduction in rice yield was due to the lower head number in AV. The reduction percentage of head number was 17.8% in AV compared with OP (normal harvest).

An AV experiment conducted by Homma et al. (2016) in Chiba prefecture using rice cultivar Koshihikari also showed the reduction in rice yield. From the simulation result, 20% of shading resulted 20% reduction of rice yield (Homma et al. 2016).

Through the field experiment and literature review results, it is undeniable that partial shading in AV had caused reduction in the rice yield. According to the guideline from MAFF (2013), criteria to measure the yield reduction in AV should be compared with “average crop yield in the same area without AV”. In some cases where the farmer manages their rice field very well, rice yields may not reduce more than 20% when compared with the average crop yield (under full sunlight) grow by rice farmers in the same area. This assumption was verified by the current AV experimental field targeted for this research.

### **5.2 Simulation approach in AV with rice cultivation**

In this study, three simulation models were applied in AV namely solar radiation (Revit & Dynamo), crop growth (APSIM-Oryza), and solar energy (PVSyst). Data from field experiment and simulation model had generated a high value of  $R^2$  which were 0.7873 (solar radiation model), 0.9832 for total biomass simulation (crop growth model), and 0.9873 (solar energy model). The high  $R^2$  explains all the variability of the response data around its mean and indicate the reliability of model. Therefore, these three models are suitable to be used in AV to estimate solar radiation, rice yield, and energy output.

### **5.3 Conclusion**

In the scenario analysis, it was concluded that economically optimum rice and energy production was at tilt angle 25° in August. However, the default tilt angle applied in Chikusei farm is 14° in August. The result provides a decision support to the farmer for considering changing the default tilt angle from 14° to 25° to gain slightly higher monetary benefit (0.06%) for both rice and energy production.

This study also produces a significant finding from the simulation approach. The research provides robust estimates of solar radiation, rice yield, and energy production through modelling approaches (Revit & Dynamo, APSIM-Oryza, and PVSyst). In conclusion, this study clearly advances current knowledge from previous published studies that were not explicitly managed to find answer for the economically optimum conditions for rice yield and energy production.

### **5.4 Recommendations and future study application**

For future study application, more scenario analysis could be carried out on other months besides August to determine the economically optimum benefit of rice yield and energy output. In addition, longer field experiment (two to three seasons) would be better to validate the field data and understand microclimate condition under AV. Larger sampling area was also suggested to improve data confident. Lately, the introduction of bifacial solar photovoltaic panels technology in the market would be worth for future investigation. Bifacial solar panel with frameless, dual-glass, and clear backsheet design to increase reflection of incoming solar radiation would be worth for future investigation (Zhu et al., 2019). Finally, it is necessary to examine not only the rice crop, but different crops should be explored to ascertain the larger potential of AV throughout Japan.

## References

- Amaducci, S., Yin, X., & Colauzzi, M. (2018). Agrivoltaic systems to optimise land use for electric energy production. *Applied Energy*, 220, 545–561. <https://doi.org/10.1016/j.apenergy.2018.03.081>
- Bouman, B. A. M., Kropff, M. J., Tuong, T. P., Wopereis, M. C. S., ten Berge, H. F. M., & van Laar, H. H. (2001). *ORYZA2000: modeling lowland rice*. International Rice Research Institute and Wageningen University and Research Centre. [http://books.irri.org/9712201716\\_content.pdf](http://books.irri.org/9712201716_content.pdf)
- Bouman, B. A. M., & van Laar, H. H. (2006). Description and evaluation of the rice growth model ORYZA2000 under nitrogen-limited conditions. *Agricultural Systems*, 87(3), 249–273. <https://doi.org/10.1016/j.agsy.2004.09.011>
- Dinesh, H., & Pearce, J. M. (2016). The potential of agrivoltaic systems. *Renewable and Sustainable Energy Reviews*, 54, 299–308. <https://doi.org/10.1016/j.rser.2015.10.024>
- Dixon, J., Li, X., Msangi, S., Amede, T., Bossio, D., Ceballos, H., Ospina, B., Howeler, R., Reddy, B. V. S., Abaidoo, R., Timsina, J., Crissman, C., Mares, V., Quiroz, R., Leon-Velarde, C., Herrero, M., Blummel, M., Holmann, F., Peters, M., White, D., Qadir, M., & Szonyi, J. (2010). *Feed, food and fuel: Competition and potential impacts on small-scale crop–livestock–energy farming systems*. [https://doi.org/10.1016/0016-2361\(89\)90029-X](https://doi.org/10.1016/0016-2361(89)90029-X)
- Dupraz, C., Marrou, H., Talbot, G., Dufour, L., Nogier, A., & Ferard, Y. (2011). Combining solar photovoltaic panels and food crops for optimising land use: Towards new agrivoltaic schemes. *Renewable Energy*, 36(10), 2725–2732. <https://doi.org/10.1016/j.renene.2011.03.005>
- Evans, L. T., & De Datta, S. K. (1979). The relation between irradiance and grain yield of irrigated rice in the tropics, as influenced by cultivar, nitrogen fertilizer application and month of planting. *Field Crops Research*, 2, 1–17. [https://doi.org/10.1016/0378-4290\(79\)90002-9](https://doi.org/10.1016/0378-4290(79)90002-9)

- Gaydon, D. S., Balwinder-Singh, Wang, E., Poulton, P. L., Ahmad, B., Ahmed, F., Akhter, S., Ali, I., Amarasingha, R., Chaki, A. K., Chen, C., Choudhury, B. U., Darai, R., Das, A., Hochman, Z., Horan, H., Hosang, E. Y., Kumar, P. V., Khan, A. S. M. M. R., Laing, A. M., Liu, L., Malaviachichi, M. A. P. W. K., Mohapatra, K. P., Muttaleb, M. A., Power, B., Radanielson, A. M., Rai, G. S., Rashid, M. H., Rathanayake, W. M. U. K., Sarker, M. M. R., Sena, D. R., Shamim, M., Subash, N., Suriadi, A., Suriyagoda, L. D. B., Wang, G., Wang, J., Yadav, R. K., & Roth, C. H. (2017). Evaluation of the APSIM model in cropping systems of Asia. *Field Crops Research*, 204, 52–75.  
<https://doi.org/10.1016/j.fcr.2016.12.015>
- Goetzberger, A., & Zastrow, A. (1982). On the coexistence of solar-energy conversion and plant cultivation. *International Journal of Solar Energy*, 1(1), 55–69.  
<https://doi.org/10.1080/01425918208909875>
- GRiSP. (2013). *Rice Almanac, 4th edition, Source Book for One of the Most Important Economic Activities on Earth*. 283.
- Heinemann, A. B., van Oort, P. A. J., Fernandes, D. S., & Maia, A. de H. N. (2013). Sensitivity of APSIM/ORYZA model due to estimation errors in solar radiation. *Bragantia*, 71(4), 572–582. <https://doi.org/10.1590/s0006-87052012000400016>
- Hirata, K. (2014). *Japan Climate Vision 2050: An energy future independent of nuclear power and fossil fuels*. <https://www.kiconet.org/wp/wp-content/uploads/2014/05/japan-climate-vision-2050-scenario-en.pdf>
- Homma, M., Doi, T., & Yoshida, Y. (2016). A field experiment and the simulation on agrivoltaic-systems regarding to rice in a paddy field. *Journal of Japan Society of Energy and Resources*, 37(6), 23–31.
- ISEP. (2018). *Share of Renewable Energy Power in Japan, 2018*.  
<https://www.isep.or.jp/en/717/>
- Kensek, K. (2015). Visual Programming for Building Information Modeling: Energy and Shading Analysis Case Studies. *Journal of Green Building*, 10(4), 28–43.  
<https://doi.org/https://doi.org/10.3992/jgb.10.4.28>

- Kimura, K. (2017). Feed-in Tariffs in Japan: Five Years of Achievements and Future Challenges. In *Renewable Energy Institute*. [https://www.renewable-ei.org/en/activities/reports/img/pdf/20170810/REI\\_Report\\_20170908\\_FIT5years\\_Web\\_EN.pdf](https://www.renewable-ei.org/en/activities/reports/img/pdf/20170810/REI_Report_20170908_FIT5years_Web_EN.pdf)
- Kumar, N. M., Kumar, M. R., Rejoice, P. R., & Mathew, M. (2017). Performance analysis of 100 kWp grid connected Si-poly photovoltaic system using PVsyst simulation tool. *Energy Procedia*, 117, 180–189. <https://doi.org/10.1016/j.egypro.2017.05.121>
- Li, T., Angeles, O., Marcaida, M., Manalo, E., Manalili, M. P., Radanielson, A., & Mohanty, S. (2017). From ORYZA2000 to ORYZA (v3): An improved simulation model for rice in drought and nitrogen-deficient environments. *Agricultural and Forest Meteorology*, 237–238, 246–256. <https://doi.org/10.1016/j.agrformet.2017.02.025>
- MAFF, J. (2013). *Farmland Conversion Guideline*. <http://www.maff.go.jp/j/nousin/noukei/totiriyo/attach/pdf/einogata-22.pdf>
- Marrou, H., Wery, J., Dufour, L., & Dupraz, C. (2013). Productivity and radiation use efficiency of lettuces grown in the partial shade of photovoltaic panels. *European Journal of Agronomy*, 44, 54–66. <https://doi.org/10.1016/j.eja.2012.08.003>
- METI. (2018). Strategic Energy Plan. In *Ministry of Economy Trade and Industry, Japan*.
- Moriasi, D. N., Arnold, J. G., Van Liew, M. W., Bingner, R. L., Harmel, R. D., & Veith, T. L. (2007). Model evaluation guidelines for systematic quantification of accuracy in watershed simulations. *American Society of Agricultural and Biological Engineers*, 50(3), 885–900. <https://doi.org/10.13031/2013.23153>
- Nagashima, A. (2005). *Sunlight Power Generation System*. *Japan Patent No. 2005-277038*, 6 October 2005.
- Nuwan, de S. (2018). *Optimizing Productivity and Quality of Wheat through Modelling Approach*. Ph.D. Thesis, Graduate School of Agricultural & Life Sciences, the University of Tokyo.
- Penning de Vries, F. W. T., & van Laar, H. H. (1982). Simulation of plant growth and crop production. In *Wageningen Centre for Agricultural Publishing and Documentation, Netherlands*.

- Saxton, K. E., & Rawls, W. J. (2006). Soil water characteristic estimates by texture and organic matter for hydrologic solutions. *Soil Science Society of America Journal*, 70(5), 1569–1578. <https://doi.org/10.2136/sssaj2005.0117>
- Sekiyama, T., & Nagashima, A. (2019). Solar sharing for both Food and clean energy production: Performance of agrivoltaic systems for corn , a typical shade-intolerant crop. *Environments*, 6(6), 1–12.
- SoilGrids. (2019). *SoilGrids*. <https://soilgrids.org>
- Soltani, A., & Sinclair, T. R. (2012). *Modeling Physiology of Crop Development, Growth and Yield*. CABI, Wallingford, UK.
- Stansel, J. W. (1975). Effective utilization of sunlight, in six decades of rice research in Texas. *Research Monograph, Texas Agricultural Experiment Station, U.S. Department of Agriculture*, 4, 43–50.
- Takahashi, Y., & Yoshida, T. (2007). Studies on delaying the transplanting time of paddy rice cultivar “Asahi-no-yume” after wheat cropping in Tomo area of Gunma prefecture. *Japanese Journal of Crop Science*, 76(3), 355–361. <https://doi.org/10.1626/jcs.76.355>
- Tuong, T. P., Marquez, J. A., Kropff, M. J., & Wopereis, M. C. S. (1994). Mechanisms and control of percolation losses in irrigated puddled rice fields. *Soil Science Society of America Journal*, 58(6), 1794–1803. <https://doi.org/10.2136/sssaj1994.03615995005800060031x>
- Valle, B., Simonneau, T., Sourd, F., Pechier, P., Hamard, P., Frisson, T., Ryckewaert, M., & Christophe, A. (2017). Increasing the total productivity of a land by combining mobile photovoltaic panels and food crops. *Applied Energy*, 206, 1495–1507. <https://doi.org/10.1016/j.apenergy.2017.09.113>
- Vergara, B. S., & Chang, T. T. (1985). *The Flowering Response of the Rice Plant to Photoperiod* (4th ed.). International Rice Research Institute, Los Banos, Philippines.
- Wang, J., Wang, E., Feng, L., Yin, H., & Yu, W. (2013). Phenological trends of winter wheat in response to varietal and temperature changes in the North China Plain. *Field Crops Research*, 144, 135–144. <https://doi.org/10.1016/j.fcr.2012.12.020>

- Yang, L., Wang, Y., Kobayashi, K., Zhu, J., Huang, J., Yang, H., Wang, Y., Dong, G., Liu, G., Han, Y., Shan, Y., Hu, J., & Zhou, J. (2008). Seasonal changes in the effects of free-air CO<sub>2</sub> enrichment (FACE) on growth, morphology and physiology of rice root at three levels of nitrogen fertilization. *Global Change Biology*, *14*(8), 1844–1853.  
<https://doi.org/10.1111/j.1365-2486.2008.01624.x>
- Yoshida, S. (1981). Fundamentals of Rice Crop Science. In *International Rice Research Institute, Los Banos, Philippines*.
- Zhu, Q., Zhu, C., Liu, S., Shen, C., Zhao, W., Chen, Z., Chen, L., Wang, J., Wang, L., Zhang, S., & Lv, J. (2019). A model to evaluate the effect of shading objects on the energy yield gain of bifacial modules. *Solar Energy*, *179*, 24–29.  
<https://doi.org/10.1016/j.solener.2018.12.006>